Wendy Nogueira

PYROLYSIS OF LIPID NANOTUBES

Short Duration Internship Supervised by Kristina Jajcevic and Professor Kaori Sugihara

AUGUST 2018
UNIVERSITE DE GENEVE – FACULTE DES SCIENCES

Table of contents

1. Introduction

Lipids are biomolecules that play major roles for living organisms. Examples include the formation of biological structures, storage of energy and signaling. One of the most important functions of lipids for eukaryote cells is the formation of the cell membrane separating the cell from its environment and delimiting the different organelles inside the cell. The ability of lipids to form this biological membrane originates from their amphiphilic character, meaning that they are characterized by a polar moiety called the polar head and a nonpolar moiety called the hydrophobic chain. In aqueous media and in specific conditions, the lipid molecules self-assemble into a bilayer so that the hydrophobic chains interact with one another to minimize the contact with the water molecules, while the polar heads interact with the water molecules through hydrogen bonds and electrostatic interactions[1].

Another important characteristic of lipids is that they are rich in carbon as their alkyl chains are only composed of carbon and hydrogen. In addition to being essential for all life forms, carbon also plays an important role in technology. Indeed, carbon is widely used in different fields for example as a source of energy, in electronics, catalysis, jewellery, etc. When the size of the material reaches the nanoscale, carbon nanomaterials show an interesting behaviour regarding their electrical, thermal, chemical and mechanical properties. Examples of this kind of materials include graphene, fullerene, carbon nanotubes, carbon dots, etc[2].

As carbon nanomaterials exhibit such interesting properties as mentioned above, this project investigates the potential application of lipids to synthesize carbon nanomaterials; more specifically, via pyrolysis of lipid nanotubes (LNTs). Being relatively cheap, rich in carbon and biocompatible, lipids could be an interesting precursor of such materials.

The properties of the lipid used for this project is discussed in section 1.1, while a small review concerning the properties and the synthesis employed nowadays to form some carbon nanomaterials is presented in the section 1.2.

1.1 1,2-dioleoyl-sn-glycero-3-phosphoethanolamine

Lipids can form bilayers in aqueous media as mentioned before. However, this kind of molecules have the ability to assemble themselves in other ways as well. The morphology of the formed aggregate depends mainly on two factors:

- the structure of the single lipid molecule
- the conditions of the solution (pH, temperature, concentration, presence of electrolytes)[3]

An interesting lipid is 1,2-dioleoyl-sn-glycero-3-phosphoethanolamine (DOPE) which possesses the ability to aggregate as LNTs under specific conditions. **Figure 1** shows its chemical structure.

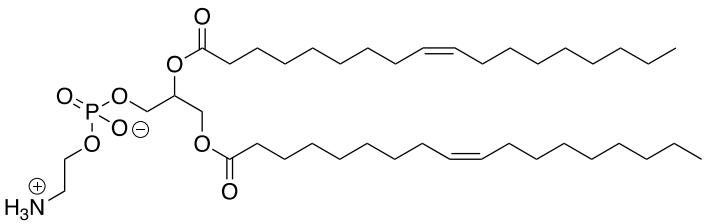

Figure 1 Illustration of the chemical structure of DOPE

In previous research conducted by Sugihara et al., it was demonstrated that DOPE self-assembles into blocks characterized by an inverted-hexagonal phase (H_{II}) under physiological conditions. The morphology of the aggregate can easily be changed through pipetting when a solution flow is generated. In fact, the lipid blocks initially formed are adsorbed on a surface functionalized with a polymer. When the solution flow is applied, parts of the blocks remain attached to the surface while other parts move apart and form interconnected tubes between the different lipid blocks. The final system contains H_{II} blocks and single-wall nanotubes, with a diameter of 19.1 ± 4.5 nm and a length close to 1 mm.[4]

The DOPE lipid was chosen as starting material for this project, not only for its biocompatibility and high percentage of carbon, which are qualities common to all lipids, but also for its specific ability to form LNTs.

1.2 Carbon nanomaterials

1.1.1 Graphene

Graphene can be synthesized by chemical vapor deposition or by mechanic exfoliation of graphite. Much research is done today on its synthesis as its physical properties are interesting. Indeed, graphene exhibits extraordinary electrical, thermal and mechanical properties, making it a material of choice for electronics.[5]

1.1.2 Fullerene

Fullerenes are mainly synthesised by vaporisation of graphite under inert atmosphere[6]. This carbon nanomaterial is poorly soluble in water. As a consequence, the synthesis of soluble fullerene derivatives attracted much attention lately for biological purposes[7]. Nowadays, fullerenes find application in various fields such as in the production of solar cells[8-9], tribology[10], bio-medicine[7], cosmetics[11], etc.

1.1.3 Carbon nanotubes

Carbon nanotubes (CNTs) synthesis has been intensively studied during these last few years, and several paths have been developed. The main techniques used are the catalysed chemical vapor deposition, the laser ablation and the carbon arc-discharge[12]. The cost of production being a major issue, much effort has been put into developing methods using cheap starting materials. For example, researches carried out by Iyuke et al. allowed the fabrication of CNTs by coal pyrolysis[13]. CNTs find applications in several fields such as batteries[14], biosensors[15], electronics[16], etc.

1.1.4 Carbon dots

Carbon dots can be synthesised by many different methods such as electrochemical synthesis, chemical oxidation or pyrolysis of organic molecules. Some methods allowing functionalization of the surface of the carbon dots have also been developed in order to modify the properties of the material such as the photoluminescence and the solubility[17]. In addition to their extraordinarily stable photoluminescence, carbon dots are biocompatible as they show a low cytotoxicity[18]. Thus, these materials have been intensively studied for biomedical imaging[19].

2. Results and Discussion

As mentioned before, the purpose of this project is to investigate the potential application of LNTs using DOPE as precursor to synthesise carbon nanomaterials. The project was divided in four parts:

- LNTs formation using DOPE
- Pyrolysis process of LNTs – Effect of temperature
- Pyrolysis process of LNTs – Effect of heating time
- Pyrolysis process of lipid blocks

The results that were obtained and the observations made throughout the project are presented in the following sections.

2.1 LNTs formation using DOPE

As a first step, LNTs were formed the same way that was proposed by Sugihara et al. during their investigation of DOPE.

The lipid solutions were prepared from a stock solution of DOPE stored in chloroform. In order to be able to image the LNTs by fluorescent microscopy, a fluorophore-tagged lipid (Rhodamine-PE) was added at a concentration of 1%. It is important to not add too much fluorophore. In fact, a too high concentration of the latter may destroy the structure of the LNTs. The solutions were then dried under vacuum for at least 2 h, rehydrated in HEPES up to a final concentration of 1mg/mL and sonicated until the lipids detached from the vial's wall. While detaching from the walls, H_{II} blocks were formed. Once, a piece of PDMS with a hole in the middle was placed at the centre of the surface to accommodate the sample; the surfaces were activated through oxygen plasma and coated with polyethylenimine. The lipid solution was added in the well and the solution was left incubated for 30 min at r.t, so the lipids could adhere to the surface. The petri dish was covered with an aluminium sheet during the incubation in order to avoid the degradation of the fluorophore which is light sensitive. After the incubation, a shear force was applied for 30-40 sec by inducing a solution flow using a pipette and the surface was washed 15 times with HEPES buffer.

The successful formation of the LNTs was confirmed by fluorescent microscopy with Nikon Eclipse Ti-E (Nikon, JP) equipped with an objective lens 40x and a fluorescent filter TRITC.

Figure 2 shows the setup of the microscope. An incident light emitted by a mercury lamp passes through a first filter called "excitation filter" in order to keep only the component of the light corresponding to the excitation wavelength of the fluorophore. The beam is then reflected on the sample by a dichroic beam splitter to excite the fluorophore. The light emitted by the sample passes through the same dichroic beam splitter and is filtered to only keep the component of the light corresponding to the emission of the rhodamine-PE.[a]

[a] https://www.jic.ac.uk/microscopy/more/T5_6.htm

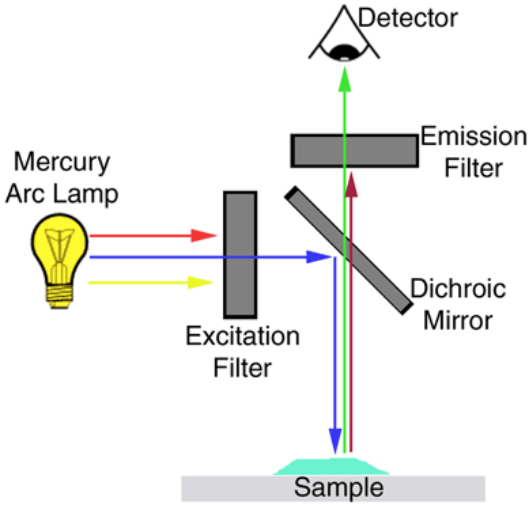

Figure 2 Illustration of the principle of a fluorescent microscope

Figure 3 shows the LNTs that are formed. The small red dots are the lipid blocks. It can be noticed that tubes originate from the lipid blocks and that they are interconnected. However, the density of the tubes on the surface is relatively low.

Before proceeding with the next steps of the project, it was preferable to establish a new protocol in order to increase this density. Indeed, the pyrolysis being a process of degradation, it is probable that only a part of the sample will be left after the heat treatment. In order to increase the chances of characterizing the sample after the pyrolysis process, a higher density of tubes is thus preferable. As the sample is in the nanoscale and thus already difficult to characterize, this is especially important in this case.

In order to increase the density, the effect of the temperature during the incubation of the lipid solution was investigated. For this purpose, the samples were prepared following the very same procedure, except that the incubation of the lipid solution on the PEI surface was performed at 55 °C instead of at r.t.

Figure 4 shows the LNTs that are formed under the new conditions. It can be noticed that the density is higher than the one obtained with the previous methodology. This phenomenon can be explained by the fact that the molecules acquire energy while increasing the temperature, which makes them more mobile. This may ease the detachment of some parts of the lipid block, leading to the formation of a higher number of tubes. However, considering the size of the structure, it would be better to start with an even higher density.

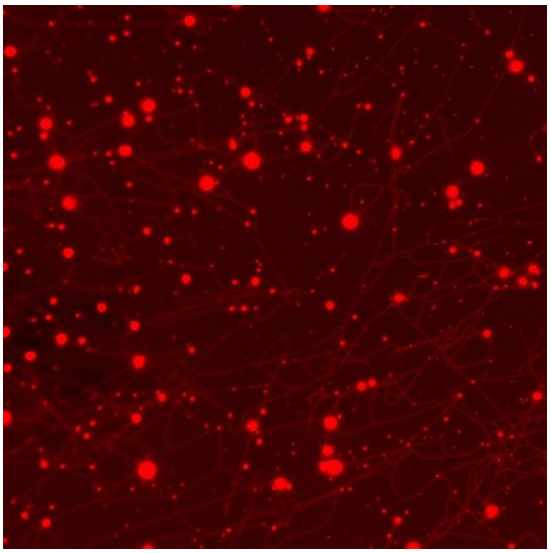

Figure 3 A fluorescent image of surface-assembled lipid nanotubes prepared without heating during the incubation step.

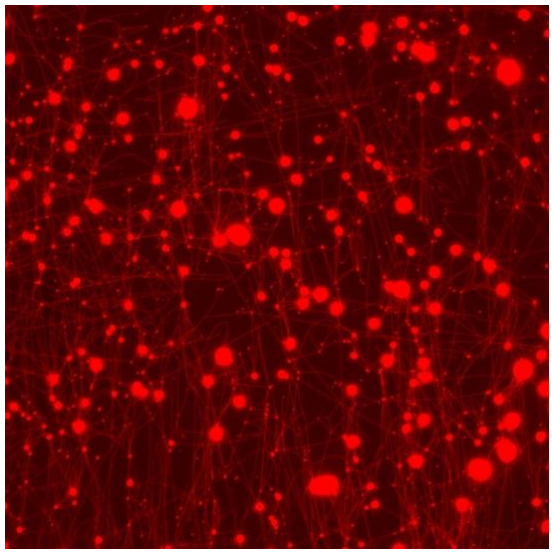

Figure 4 A fluorescent image of surface-assembled lipid nanotubes prepared by heating at 50 °C during the incubation step.

In order to increase the density of the tubes at the surface, the affinity between streptavidin and the biotin was used. Both of these molecules bind with an association constant of 10^{15}, which is the strongest interaction reported in nature at the moment. The strong affinity between them is due to several factors:

- The shape of biotin is complementary to the binding pocket of streptavidin.
- Many hydrogen bonds are formed when biotin accommodates itself in the binding pocket.
- Van der Waals interactions take place between different amino acids in the binding pocket.
- When biotin binds to streptavidin, a conformational change occurs: a flexible loop moves to link two β-sheets which locks biotin in the pocket, and prevents its removal. This mechanism is called "protein encapsulation".[20]

The strong affinity between these two molecules has already been used in a more recent research conducted by Sugihara et al. to form LNTs. The methodology proposed during the aforementioned research was used in this project.

The lipid solution was prepared from stock solutions of DOPE and DOPE-Biotin, both stored in chloroform. Both solutions were added in the same vial respectively in a ratio 96:4. In order to be able to image the LNTs by fluorescent microscopy, a rhodamine-PE was added at a concentration of 1% as previously. The lipids were dried, rehydrated in HEPES and then sonicated. The surfaces were activated, featured by a piece of PDMS with a well, functionalized by adding the PLL-*g*-PEG/PLL-*g*-PEG-Biotin solution that was left incubated for 30 min at r.t. and then washed with milli-Q water. The streptavidin solution (50 μL/ml in H_2O) was added, followed by 30 min of incubation at r.t.. The surface was washed 15 times with milli-Q water again. Then the lipid solution was added in the well, and the solution was left incubated for 30 min at 55 °C. Finally, a shear force was applied by inducing a solution flow, the surfaces were washed and the success of the LNTs formation was confirmed by fluorescent microscopy.[21]

Figure 5 shows the LNTs that are formed under these new conditions. It can be observed that it is difficult to see any tubes at first sight due to the strong fluorescence emanating from the

blocks. However, this high intensity confirms that at least more lipid blocks are attached to the surface than previously. By zooming on zones where scratches are present, the tubes become visible, which confirms the successful formation of the LNTs, and a satisfactory density is observed.

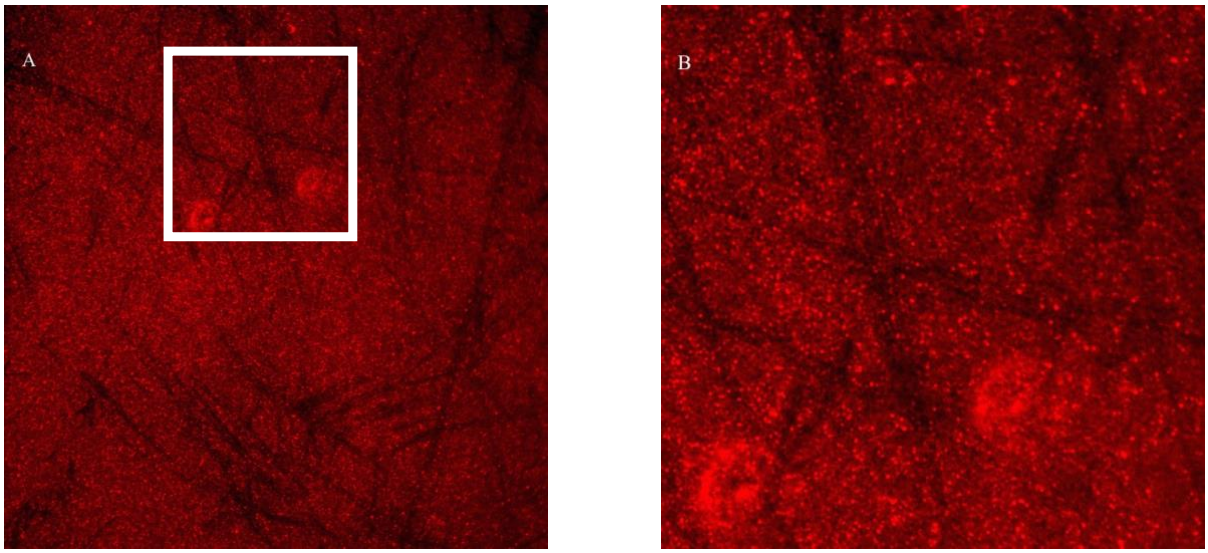

Figure 5 A fluorescent image of surface-assembled lipid nanotubes prepared with streptavidin and biotin A) full image and B) zoom on a scratch making the LNTs more visible.

A higher density is observed because the presence of streptavidin and biotin increases the affinity of the lipids for the surface which increases the number of absorbed lipid blocks. In fact, the surface is functionalized with PLL-*g*-PEG/PLL-*g*-PEG-Biotin, meaning that biotin molecules are exposed to the outside. The added streptavidin strongly bonds to the biotin located at the surface of the polymer layer. Then, the lipid blocks presenting biotin molecules at the surface are added. These biotin molecules are highly attracted to the streptavidin attached to the surface, resulting in a strong and stable adsorption of the lipid blocks. The formation of the LNTs is also facilitated in this case due to the fact that, when a part of the lipid block moves apart while applying the shear force, the biotin at the surface binds to the exposed streptavidin, which stabilizes the tube. **Figure 6** shows the different layers composing the sample.

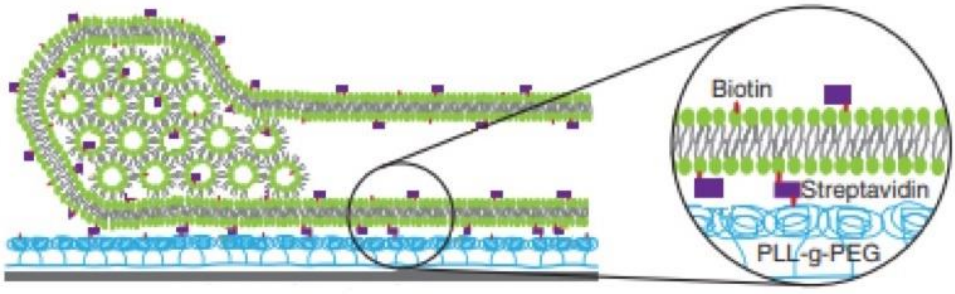

Figure 6 Illustration of the sample composition[21] (modified)

This methodology makes it possible to have a satisfactory density of LNTs. However, there is a major disadvantage when proceeding this way compared to the first methodology. Indeed, the goal of this project is to investigate the efficiency of LNTs to form carbon nanomaterials via pyrolysis. By following this protocol, the formed samples are composed of a polymer layer, a streptavidin-biotin complex layer and a final layer made of lipid blocks connected by tubes as

mentioned above and shown on **Figure 6.** The lipidic layer is rich in carbon, but the two first layers composed of polymer and streptavidin-biotin are so as well. The carbon coming from these two layers can also react during the pyrolysis process and reorganize itself to form a new kind of structure. The same observation can be made for the lipid blocks. Thus, that extra carbon may interfere during the process, and it might be difficult to say if the possibly formed carbon structures are composed of the carbon of the LNTs or not. Despite this disadvantage, this methodology was employed for the rest of the experiments in order to increase the chances to characterized the sample after heat treatment.

Once the formation of LNTs was confirmed, the samples were fixed to preserve them from any structural changes or possible degradation. Chemical fixation is a common process used in biology, especially for microscopy. Chemical agents that are capable of binding covalently specific groups are used to keep the structure as close to their natural state as possible. Glutaraldehyde and osmium tetroxide were used to fix the samples in this project. Glutaraldehyde is a di-aldehyde that condenses amines groups through a Mannich-type reaction and reductive amination, allowing the cross-linking of the head group of the lipids[22]. The osmium tetroxide is known to react with the double bonds, such as the ones presented on unsaturated fatty acids. This reagent leads to the cross-linking of the hydrophobic chains of the lipids[23]. The combination of these two chemical reagents ensures that the structure of the sample is conserved as much as possible. This process degrades the fluorophore, which means that the sample cannot be analysed by fluorescent microscopy anymore. Thus, the successful fixation of the prepared samples on silicon wafer was verified by electron microscopy.

2.2 Pyrolysis process – Effect of the temperature

As a second step, the effect of temperature on the LNTs was investigated by treating the samples by pyrolysis. Pyrolysis is a process implying the exposition of the sample to very high temperatures leading to the decomposition of organic material in new compounds that are generally enriched in carbon. The reaction is done in inert atmosphere in order to avoid an eventual oxidation of the sample or its combustion.

The choice of temperatures for this work was limited by the properties of the surfaces used to prepare the samples. The three types of surfaces chosen were glass, silicon nitride and silicon wafer. They can respectively endure 500 °C[b], 1000 °C[c] and 1414 ° C[d]. In view of this, the temperatures chosen to treat the samples were 500 °C, 800 °C and 1000 ° C.

The reactions were performed with two different furnaces for a question of availability. **Figure 7** shows the different thermal cycles. The experiment at 500 °C was conducted under nitrogen atmosphere in the furnace located in the department of physical chemistry. The samples were heated at 100 °C/h until reaching 500 °C, maintained at this temperature during 1 h and cooled to r.t by decreasing the temperature of 100 °C/h. Regarding the experiments at 800 °C and 1000 °C, they were both conducted under argon atmosphere in one of the furnaces located in the department of quantum matter physics. For the experiment performed at 800 °C, the samples were heated at 1050 °C/h until reaching 700 °C, 600 °C/h until reaching 800 °C, heated during 1 h at this temperature, and the furnace was turned off right after to cool down the sample as quickly as possible. For the experiment performed at 1000 °C, the samples were heated at 900

[b] https://www.tedpella.com/histo_html/coverslip-info.htm
[c] https://www.emsdiasum.com/microscopy/products/grids/sin_window.aspx
[d] https://www.americanelements.com/silicon-wafer-7440-21-3

°C/h until reaching 900 °C, 600 °C/h until reaching 1000 °C, heated during 1 h at this temperature, and the furnace was turned off.

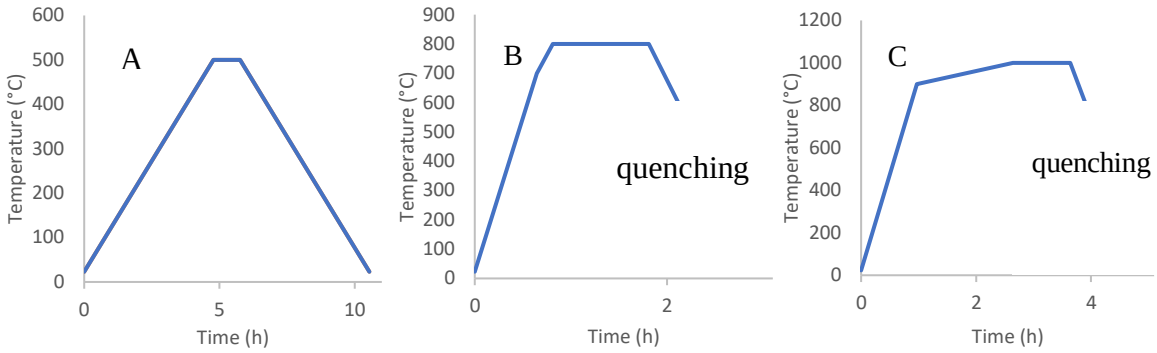

Figure 7 Illustration of the thermal cycle of the sample heated at A) 500 °C B) 800 °C C) 1000 °C

After pyrolysis, the morphology and the composition of the samples were characterized by various techniques.

2.3.1 Transmission electron microscopy and Scanning electron microscopy

The structure of the samples prepared on silicon nitride was imaged by transmission electron microscopy (Tecnai G2) before and after pyrolysis, while the samples prepared on silicon wafers were imaged by scanning electron microscopy (Jeol 6510LV) before and after pyrolysis.

Figure 8 shows the setup of these two microscopes. Regarding the transmission electron microscope (**Figure 8A**), an electron beam is formed by a tungsten filament heated through the application of a voltage. This beam is focused on the sample by magnetic lenses. The beam coming out of the sample is then focused on a screen using lenses. When the beam goes through the sample, they interact with each other, which generates an amplitude and a phase change of the electron wave according to the nature and the thickness of the sample. These changes of the properties of the electromagnetic wave are respectively responsible for the amplitude contrast and phase contrast of the image. The amplitude contrast is due to the loss of some electrons during the interaction. That loss can occur due to the absorption of the electrons by the sample and to the scattering of the electrons during the interaction. Thus, heavy objects appear darker on the image, because the electrons are scattered at larger angles and do not reach the detector, which explains why such regions have low intensity. The LNTs are mainly composed of light atoms such as carbon. However, they can be observed by this technique in this case due to the presence of osmium in the structure, which was incorporated during the fixation step.

Regarding the scanning electron microscope (**Figure 8B**), the principle of the microscope is similar to the first one. An electron beam is generated by ejecting electrons from a tungsten filament through applying a voltage. The electron beam passes through an anode to accelerate the electron. The beam is then focused on the sample with a magnetic lens, and scans the specimen over small zones. The interaction between the electrons and the sample leads to the emission of electrons at low energy located at the surface of the sample. These electrons, called secondary electrons, are accelerated toward a detector to determine the topology of the surface[24].

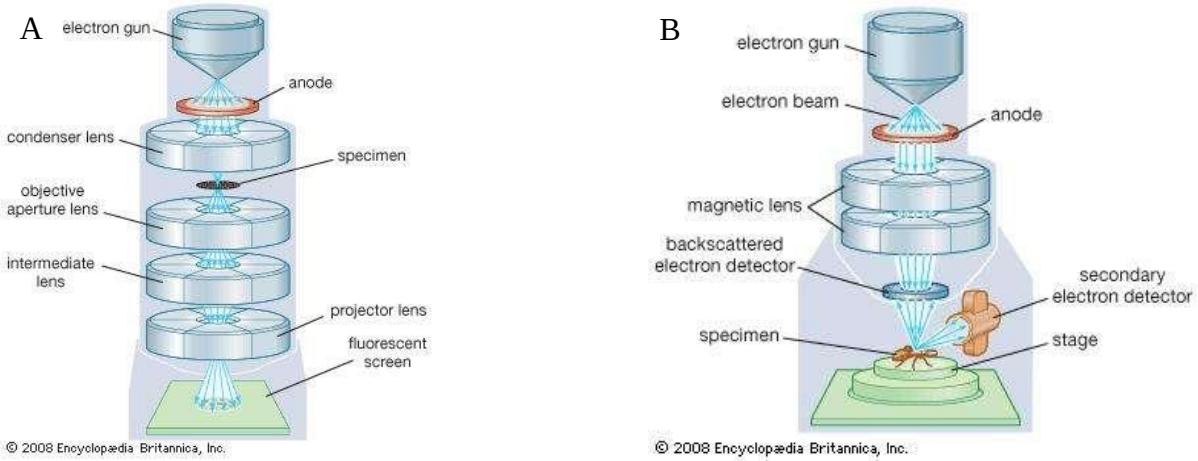

Figure 8 Illustration of the setup of A) a transmission electron microscope B) a scanning electron microscope

Figure 9 shows transmission electron microscopy (TEM) (**Figure 8A and 8B**) images and scanning electron microscopy (SEM) images (**Figure 8C and 8D**) of the non-heated samples. The same observations can be made for both types of imaging.

In both cases, LNTs are present and interconnected trough lipid blocks that are visible as well, which confirms that the fixation was successful. The network formed by the LNTs is observable over the whole surface, meaning that the density is good.

Regarding the SEM images, the tubes' network is visible when the sample is non-coated and coated with gold. However, when the sample is non-coated, a larger voltage is needed to have a well resolved image. This is an inconvenient because, in that case, the electron beam degrades the sample by burning it. This effect gets more important as the voltage is increased. Despite this disadvantage, it is preferable to not coat the samples, so that they can be analysed by other methods later, as only a few samples can be pyrolysed simultaneously because of the furnace's size.

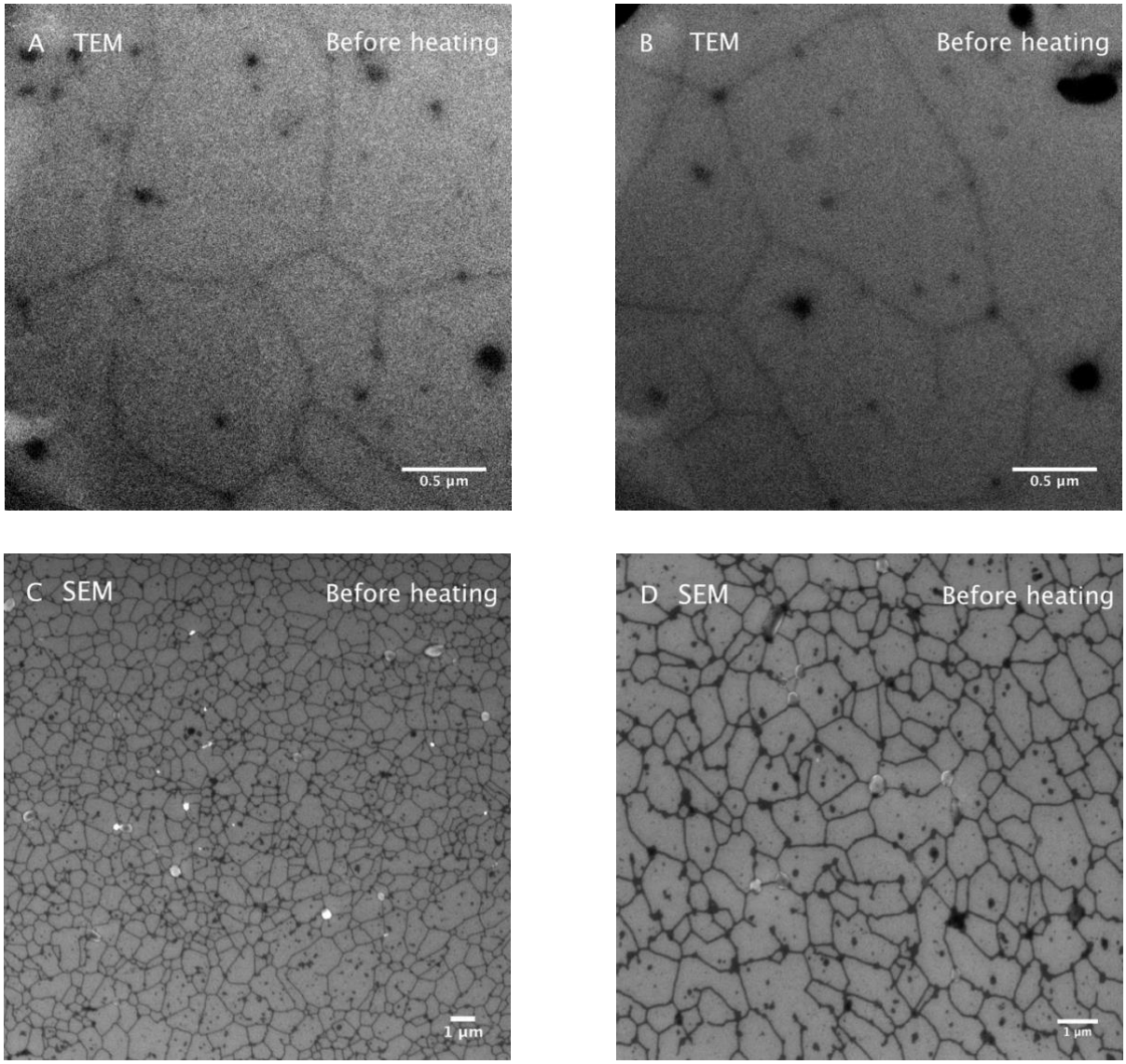

Figure 9 Transmission electron microscope images A) and B) and scanning electron microscope images C) and D) of the samples before heating.

Figure 10 shows transmission electron microscopy (TEM) images and scanning electron microscopy (SEM) images of samples heated at 500 °C for 1 h.

The results obtained by TEM (**Figure 10A and 10B**) and SEM (**Figure 10C and 10D**) are comparable. No major change is visible compared to the non-heated samples: the system is still organized as a network formed by LNTs interconnected by lipid blocks. However, the apparition of small dark dots between the tubes is observed by TEM and SEM. These are probably ashes coming from the oven that have settled on the surface. Otherwise, the shape and the density is similar.

Thus, the conditions provided by this temperature combined with this heating time seem to be soft enough for the sample as the organization of the atoms does not seem altered.

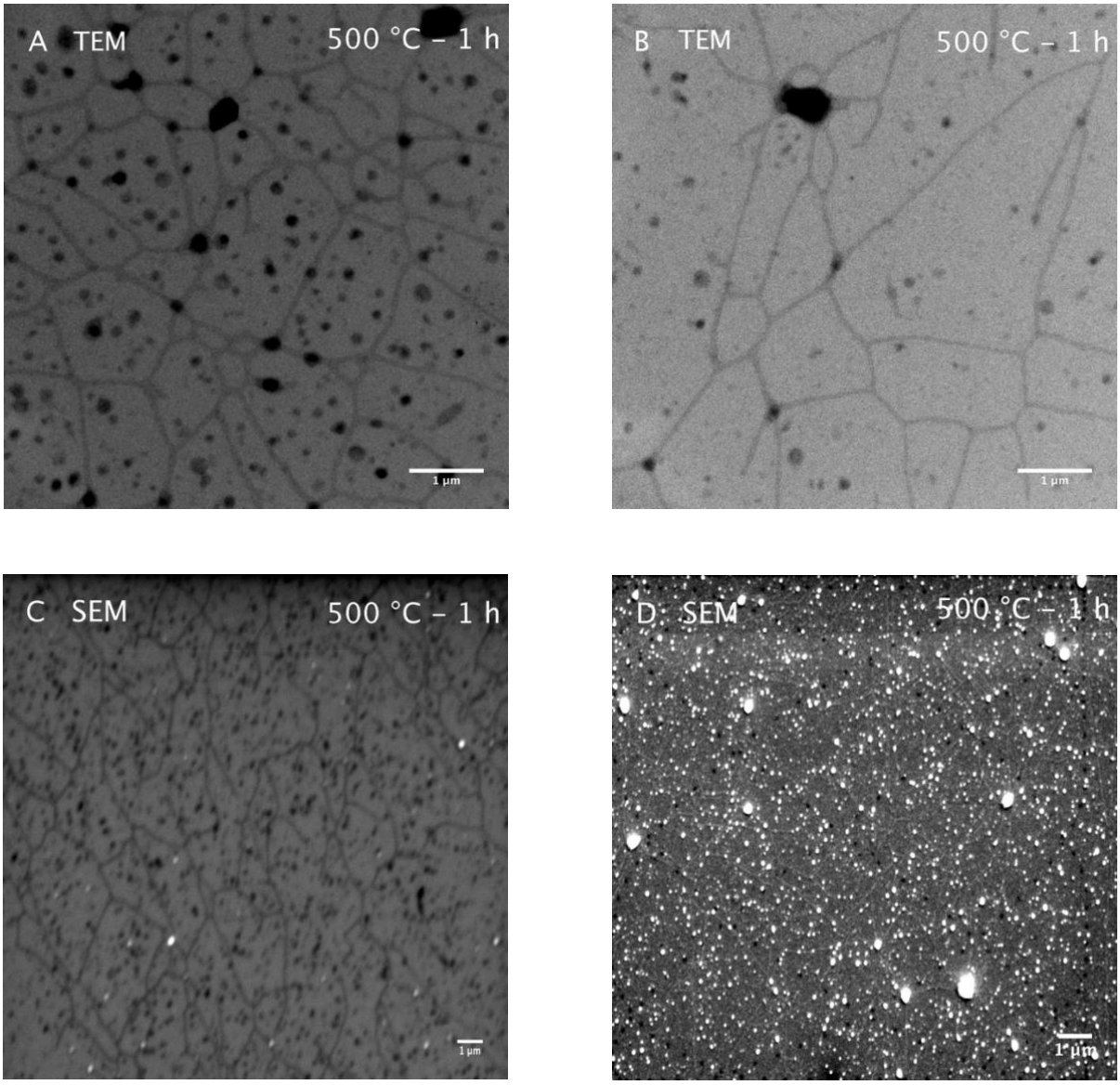

Figure 10 Transmission electron microscope images A) and B) and scanning electron microscope images C) non-coated and D) coated of the samples after a heating process at 500 °C for 1 h.

Figure 11 shows scanning electron microscopy images of samples heated at 800 °C for 1 h. The sample prepared on a TEM grid was not imaged because the grid broke, so unfortunately no TEM analysis could be performed for this set of samples.

Regarding the results obtained by SEM, the system was found to be inhomogeneous. Indeed, different regions are visible in this case. In some zones, well shaped tubes interconnected through lipid blocks are visible with a density comparable to the initial one (**Figure 11A**). In another region, the location of the LNTs is still visible but the tubes are disconnected in small fragments (**Figure 11B**). Also, a zone where the LNTs were present was found, but by looking closer at the lipid block, a structure different from the usual one is observed (**Figure 11C**). This structure is not quasi-spherical as the initial ones, but rather elongated and seems to be rolled up on itself.

Thus, it seems that part of the LNTs remain intact under these conditions, while some of them adopt a new structure.

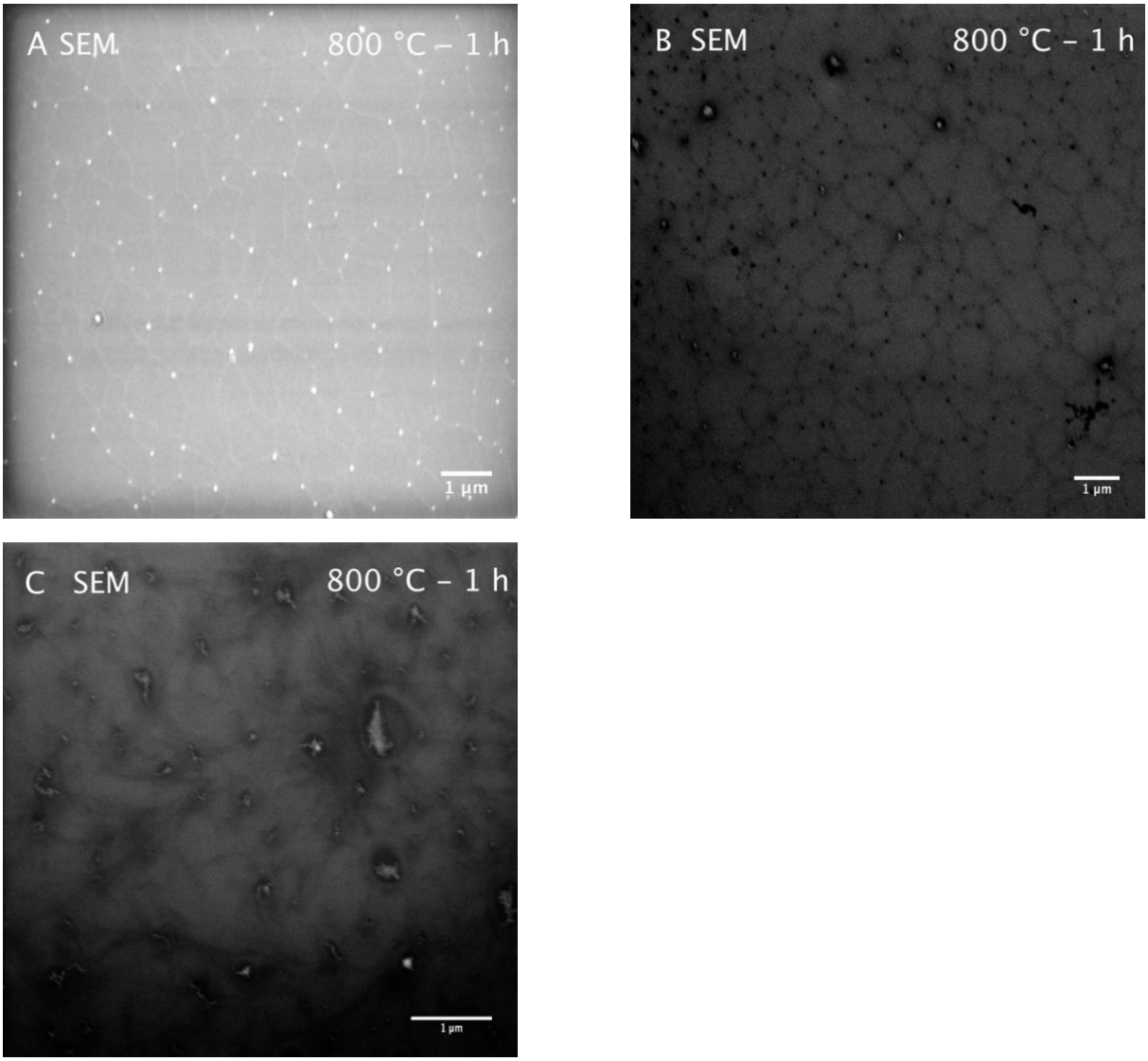

Figure 11 Scanning electron microscope images of different regions of the sample after a heating process at 800 °C for 1 h.

Figure 12 shows transmission electron microscopy (TEM) images and scanning electron microscopy (SEM) images of samples heated at 1000 ℃ for 1 h. For this set of samples, the results are completely different from the ones obtained for the other sets.

Regarding the images obtained by TEM, it is observed that no LNTs are visible anymore. Instead of that, a network formed by small elongated structures placed next to each other is observed (**Figure 12A**). That network is observable all over the surface, and seems to be located where the initial LNTs' network was. By looking more closely at one of these structures, it can be observed that it is much thinner than the LNTs and it seems to be folded on itself (**Figure 12B**). This structure is similar to the one observed by SEM for the sample heated at 800 ℃ for 1 h.

This structure appears much darker than the initial LNTs. An explanation for this phenomenon could be the fact that some material was lost as the sample is degraded during the pyrolysis process, making the system lighter. However, the structure being more compact, as it seems folded on itself, it would result in the compound having a higher mass per unit of volume, and so it would appear darker.

For ulterior experiments, a major modification could be considered during the preparation of the samples. Indeed, in this case, the LNTs were prepared on a thick TEM grid of 200 nm, which is about 10 times thicker than the LNTs. In order to improve the quality of the analysis, future samples could be prepared on a thinner TEM grid, i.e. 50 nm, 20 nm or 8 nm. These values are more comparable to the diameter of the nanotubes, and would therefore be more suitable for imaging. The disadvantages of such grids are their price and the fact that they are difficult to handle: as the membrane forming the grids is really thin, it can break more easily.

Concerning the images obtained by SEM, structures that are similar to tubes are visible all over the surface (**Figure 12C**) at first sight. However, if one looks more closely by zooming, it can be observed that there are no tubes, but only fragments. These fragments are small successive structures that are folded on themselves. They are located in what seems to be the inside of the initial tubes (**Figure 12D**). These structures are similar to the ones observed by TEM imaging. These images confirm that the compact structures are located inside the former tubes, meaning the LNTs are changed in such conditions, but no structure related to carbon nanomaterials is found.

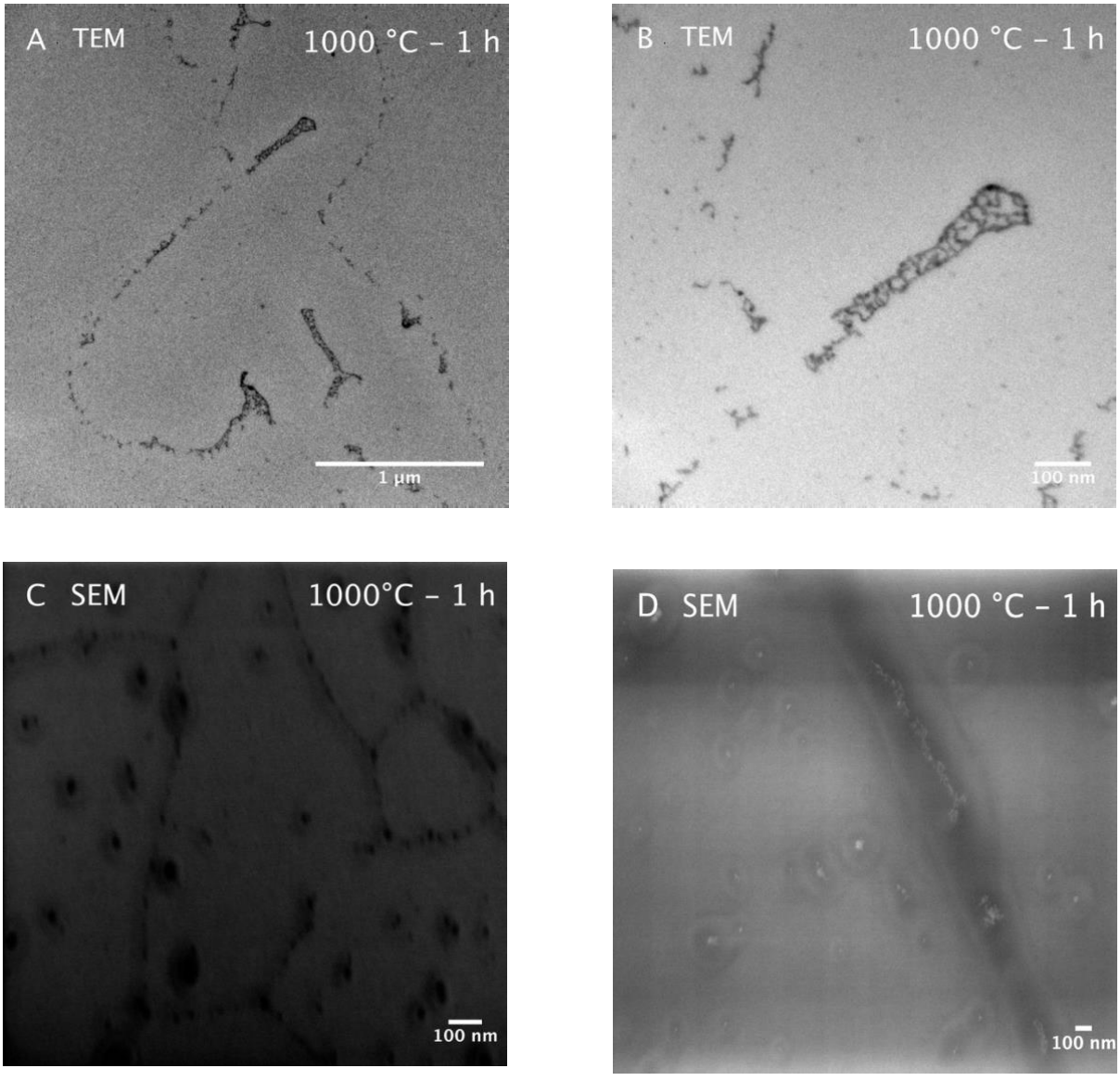

Figure 12 Transmission electron microscope images A) and B) and scanning electron microscope images C) non-coated and D) coated of the samples after a heating process at 1000 °C for 1 h.

After comparing the structural change occurring through the pyrolysis process, a change in the composition should also be investigated. In fact, even if the structure obtained after heating the sample at 500 ° during 1 h is comparable to the one of the non-heated sample, it does not mean that the composition is similar as well. In the case of the sample heated at 800 °C and 1000 °C, a different composition is expected for both cases.

This part is the most challenging one: the sample being in the nanoscale, and the concentration being quite low, it is probable that it will be difficult to obtain a significant signal.

2.3.2 Raman spectroscopy

To investigate the composition, a sample was at first analysed by a non-destructive method called "Raman spectroscopy". The principle is the following: the sample is irradiated with a light beam. The electric field of this beam exchanges energy with the vibrations of the molecules located at the surface of the sample, resulting in a change of the frequency of the initial beam. So, the difference of frequency between the initial beam and the scattered beam corresponds to a vibrational frequency, which is specific for each functional group. Thus, the sample composition at the surface can be investigated. However, not all the vibrations are detected, there is a selection rule: only the vibrations implying a change of the polarizability along the Cartesian coordinates are observable, which means that some information can be missed[25].

Figure 13 shows the Raman intensities according to the obtained Raman shift for a non-heated sample and the sample heated at 500 °C during 1 h. It can be observed that both signals are similar. A small difference is observable around 385 cm^{-1} and 1683 cm^{-1}. However, the intensities are quite low. So, it is difficult to say if this difference comes from the samples themselves or if it is due to the noise. Indeed, the main disadvantage of this method is that the Raman effect is a weak one; there are approximately 1 Raman photon for approximately a flux of 1 million photons. Additionally, the sample is in the nanoscale, so there is little material on each surface. As the intensity is proportional to the concentration, the peak's heights are small; almost at the same level as the base line. Thus, the spectra can't be analysed in a significant way.

In light of this situation, the samples heated at 800 °C and at 1000 °C have not been analysed. In fact, the temperature being relatively high, an even smaller concentration is expected, meaning the signal would be less intense. To perform this experiment, it is essential to increase the material quantity at the surface. However, the first step of this project was to develop a methodology to have a density and so a concentration in material that was high enough to perform the experiences to characterize the sample, and the protocol that was used is already the one developed to give the highest density. Thus, another more suitable method should be used for such samples.

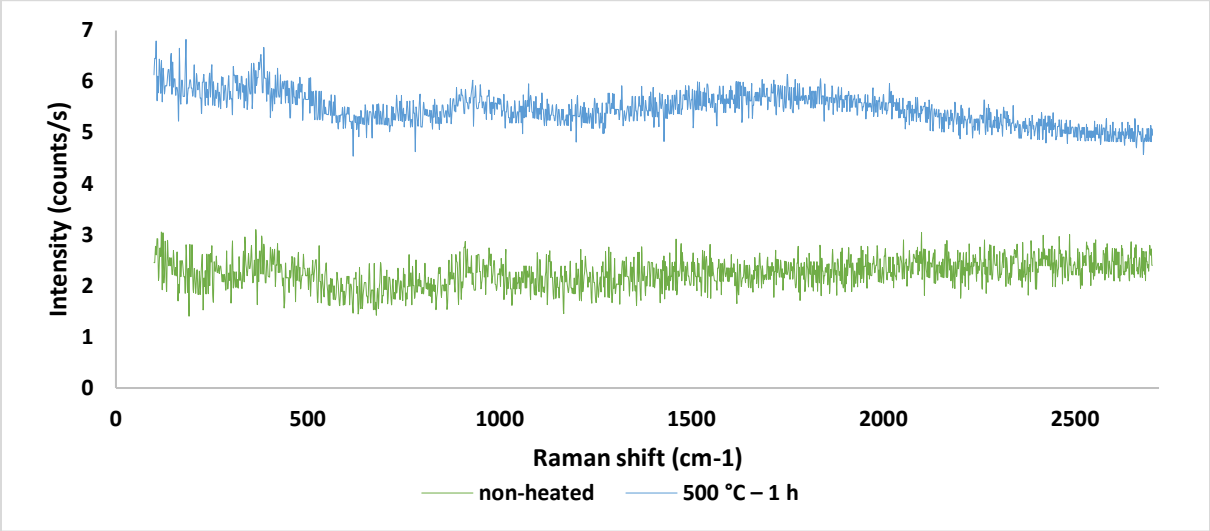

Figure 13 Raman analysis of the non-heated sample in green and the sample heated at 500 °C during 1 h in blue.

A suitable method for such samples that is based on Raman spectroscopy is the technique called Tip enhanced Raman spectroscopy (TERS). This method combines atomic force microscopy (AFM) and Raman spectroscopy. A metallic tip scans the sample to image it and the Raman shift is measured at the same time. The signal is locally amplified due to the presence of the metallic tip whose electrons are free, and so start to vibrate once they get excited due to the light beam used to do the Raman measurement. These vibrations generate a localised dipole moment that enhances the electric field at the position of the tip, resulting in an increase of the Raman signal at this exact position[26]. The samples were sent to the company for testing and the results should arrive soon.

2.3.3 Crystallography

To investigate the change of structure and composition, the sample was analysed by crystallography. The principle is the following: the sample is irradiated with an X-ray beam which is diffracted by the atoms constituting the sample. The pattern of diffraction, the angle of diffraction and the intensity of diffraction are recorded. Each atom having its own scattering power, the structure can then be reconstructed using the recorded information and an algorithm[27].

To analyse the samples, a powder experiment was performed as the system is not a mono-crystal. As the signal was relatively low and in order to increase the intensity of the signal, each measurement lasted one night. As the position of the surface affects the measurements, it is important that all the surfaces are placed exactly the same way. However, this being difficult to achieve, the height of the platform on which the samples were placed was controlled to minimize this perturbation and to make sure it was the same for all the measurements.

The sample heated at 500 °C and prepared on silicon wafer was not analysed because it was coated with gold for imaging. The gold film would have disrupted the analysis and the results would probably not have been reliable.

Figure 14 shows the intensity of the diffraction as a function of 2 theta for all the samples prepared on silicon. Major part of the peaks present for the non-heated sample and the sample heated at 800 °C are the same as the ones present for the bare surface of silicon, this means that most of the peaks are due to the surface itself and not to the sample. A small difference is

observed at an angle of 31.80 degrees; this peak is only present for the non-heated sample, meaning that this peak is specific to LNTs. The fact that this peak is missing for the sample heated at 800 °C shows that the structure and/or the composition is changing. The change of the morphology is actually confirmed by the SEM and TEM images, but no information about the composition can be determined at this point.

Regarding the sample heated at 1000 °C, the diagram is completely different from the other ones, meaning that the structure and/or the composition is different for this set of samples. The peak at 31.80 degrees is not present neither for this sample. It shows that the LNTs network probably experiences at least a modification of the atomic organisation and/or composition through the heating process. It can be noticed that even the peaks coming from the surface are not present, showing that the structure and/or composition of the surface itself is affected by the heating process as well.

By taking a closer look at the intensities at lower angles (**Figure14B**), it can be noticed that the pattern is relatively different for the four samples. Thus, measurement at lower angles is more suitable for such samples. Unfortunately, the instruments available at the University of Geneva is not appropriate for this kind of measurements. Thus, this analysis is not complete; additional measurements at lower angles are needed to make the results more relevant.

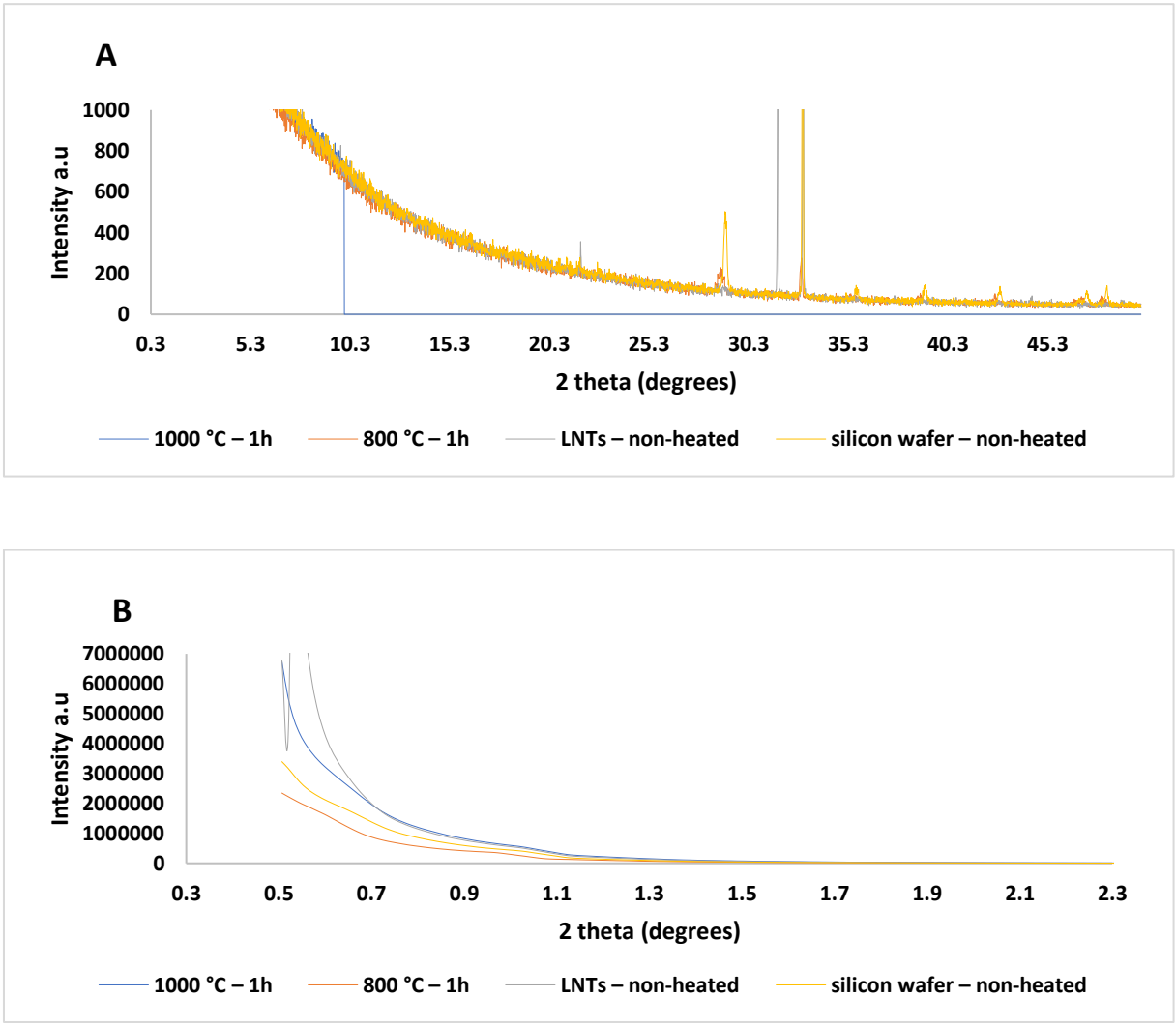

Figure 14 XRD patterns of the different samples prepared on silicon wafer A) at all angles B) only at low angles

Figure 15 shows the XRD analysis for the samples prepared on glass. In light of the melting point of the glass coverslip, only the 500 °C heating treatment was performed on this surface.

It can be observed that the pattern of diffraction is the same for the glass coverslip, LNTs and the heated LNTs, meaning that the signal is mainly due to the surface itself and not to the sample. However, at small angles (**Figure 15B**), a neat difference is visible for the sample heated at 500 °C compared to the two other ones, showing a change of structure and/or composition through the heating process. By TEM and SEM imaging, it was confirmed that the morphology was not or little affected by the heating process, so it can be expected that this difference is mainly due to a change in the composition. However, even small atomic rearrangements that are not visible with such imaging technique may occur and affect the XRD pattern.

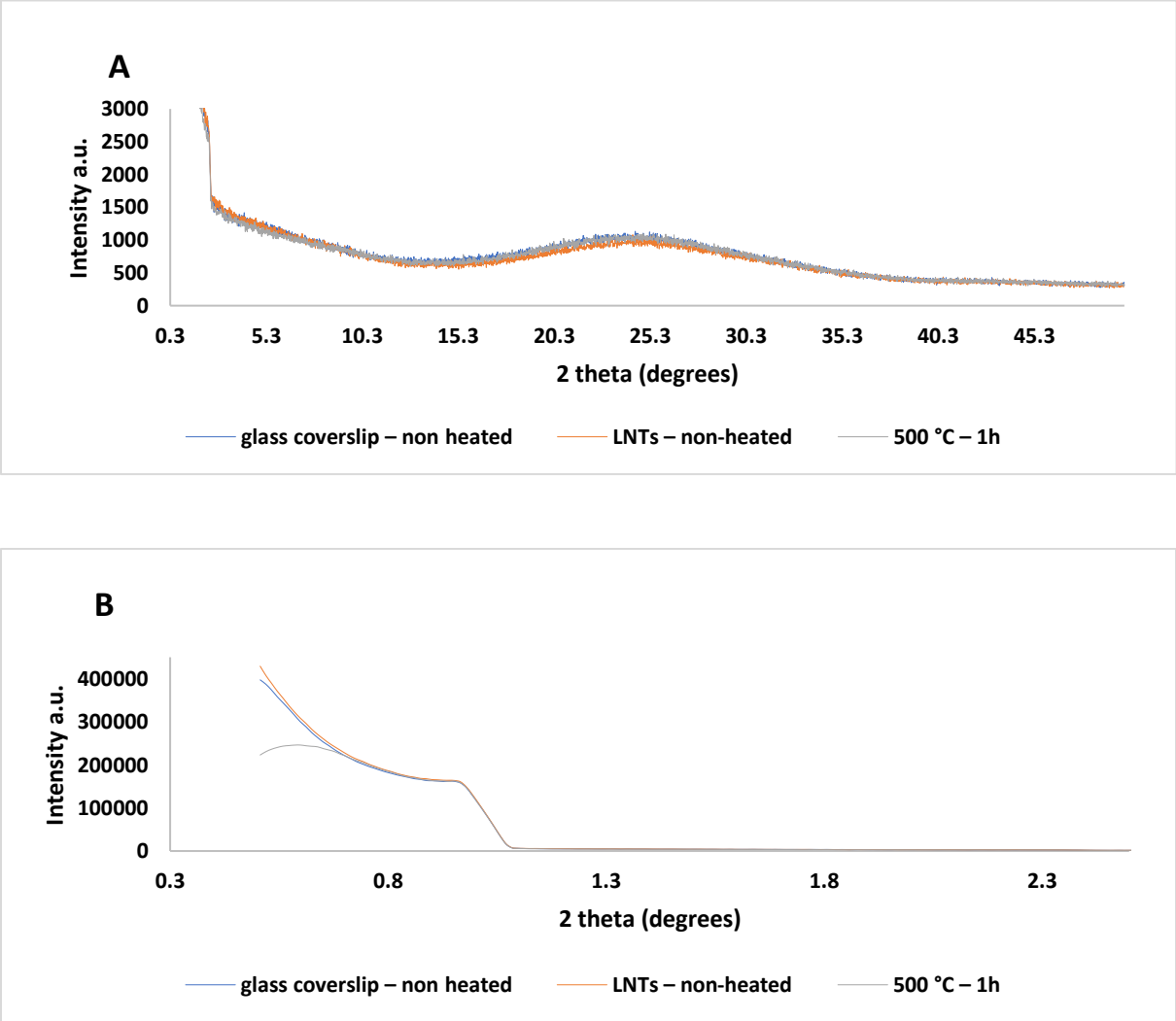

Figure 15 XRD patterns of the different samples prepared on glass A) at all angles B) only at low angles

Thus, by this characterization method, it has been confirmed that structural and/or composition changes occur via pyrolysis process. However, no further information can be provided by this analysis as the instrument does not allow measurement at lower angles.

2.3.5 Scanning electronic microscopy with Energy Dispersive X-Ray

To investigate the composition, scanning electronic microscopy with energy dispersive X-Ray (SEM-EDX), a surface specific method, has been used. This method uses a SEM microscope as electron source. These electrons interact with the atoms at the surfaces and eject electrons from the core of the atoms located at the surfaces. This phenomenon is called the photoelectric effect. Through this process, a vacancy in the electronic shells is generated. To stabilize the atoms, electrons at higher energy will fill the hole. The excess of energy can either be used to eject a new electron, called the Auger electron, or it is released as a photon. The last phenomenon is of interest in this case. This photon has an energy which is atom and shell specific, which allows the determination of the relative composition of the surface. The sample being located at the surface of the silicon wafer, its composition can be investigated specifically[28].

To perform the analysis, even though it is a qualitative one, an acceleration voltage of 15 kV and a working distance of at least 15 mm are needed in order to have a reliable analysis. This means that the obtained percentages are not exact, but they give an order of magnitude. As the distance of the plate from the beam's source can affect the detection, all the samples were analysed together the same day to make sure that the distance was the same for all of them. For each sample, three different regions of the sample have been measured in order to take an average.

As the sample should normally contain carbon, oxygen, nitrogen and osmium, these four elements were targeted for the analysis. Non-heated LNTs, LNTs heated at 800 °C and at 1000 °C for 1 h have been analysed to compare the relative atomic ratios of the atoms mentioned above. Unfortunately, the sample heated at 500 °C could not be analysed because it has been coated for the previous imaging analysis.

Figure 16 shows the atomic ratios obtained by SEM-EDX analysis for the different samples. It can be observed that before the heat treatment, the samples are quite rich in carbon and in oxygen. This observation was expected as DOPE, the lipid constituting the LNTs, is mainly composed of carbon and oxygen. However, quite surprisingly, no nitrogen and osmium are detected, although nitrogen is present in DOPE and osmium is added during the fixation step. This might be due to the fact that the percentage of nitrogen and osmium might be so small that the instrument was not sensitive enough to detect them, due to the intense signal rising from the carbon and oxygen.

By comparing the composition of the sample before and after the heating process, it can be noticed that the sample is not enriched in carbon, as expected, but in oxygen. It is also observed that this phenomenon increases along with an increase of the temperature. In fact, after being heated at 800 °C for 1 h, the atomic ratio of the oxygen rises from 22.71 ± 1.97 % to 60,57 ± 5.11 %, and to 61.55 ± 0.37 % after being heated at 1000 °C for 1 h. These results were unexpected as the experiments were performed under inert atmosphere (Argon).

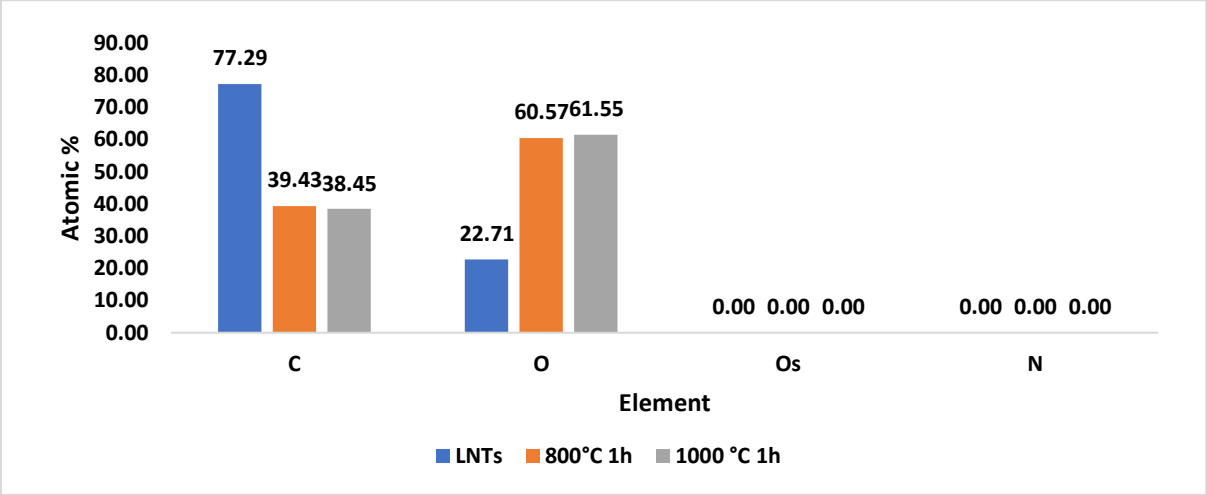

Figure 16 Atomic ratio of carbon, oxygen, osmium and nitrogen of the different samples determined by SEM-EDX analysis

A hypothesis to explain the origin of this oxygen is that the surface itself, so the silicon wafer, contains oxygen that is liberated during the heating process. Indeed, it is known that a layer with a thickness of up to 1-2 nm of silicon dioxide is formed when the silicon wafer is exposed to oxygen. The atmosphere containing oxygen contaminates the wafer that way. Also, the surface is activated through oxygen plasma, meaning that some oxygen could have been inserted during that step as well[27]. Through heating, this oxygen might be liberated and react with the sample.

At room temperature, oxygen is in a triplet state, meaning that the oxidation of organic matter is hindered due to the high energetic barrier related to the reaction. However, at high temperature, the oxygen molecules get excited and go from a triplet state to a singlet state. In this latter state, the oxygen molecules can react much easily with organic matter, resulting in the oxidation of the subtract. The greater the temperature, the greater the number of excited oxygen molecules, meaning that the probability of encountering the sample and to react with it increases. This could explain this strangely high percentage of oxygen, and the percentage increasing along with the temperature.

In order to confirm this hypothesis, a SEM-EDX analysis has been performed on the edges of the silicon wafer containing the samples treated with heat. **Figure 17** shows the atomic ratios of oxygen of the bare surfaces non-treated and treated with heat.

It can be observed that the atomic ratio of oxygen at the surface of the silicon wafer increases with the applied temperature. In fact, the non-heated surface has an atomic ratio of oxygen of 0.59 ± 0.16 %, while the one heated at 800 °C and 1000 °C for 1 h have respectively an atomic ratio of 6.93 ± 1.18 % and 11.23 ± 3.68 %. Thus, it is confirmed that the oxygen located at the surface of the silicon wafer is related to the temperature applied for the pyrolysis process.

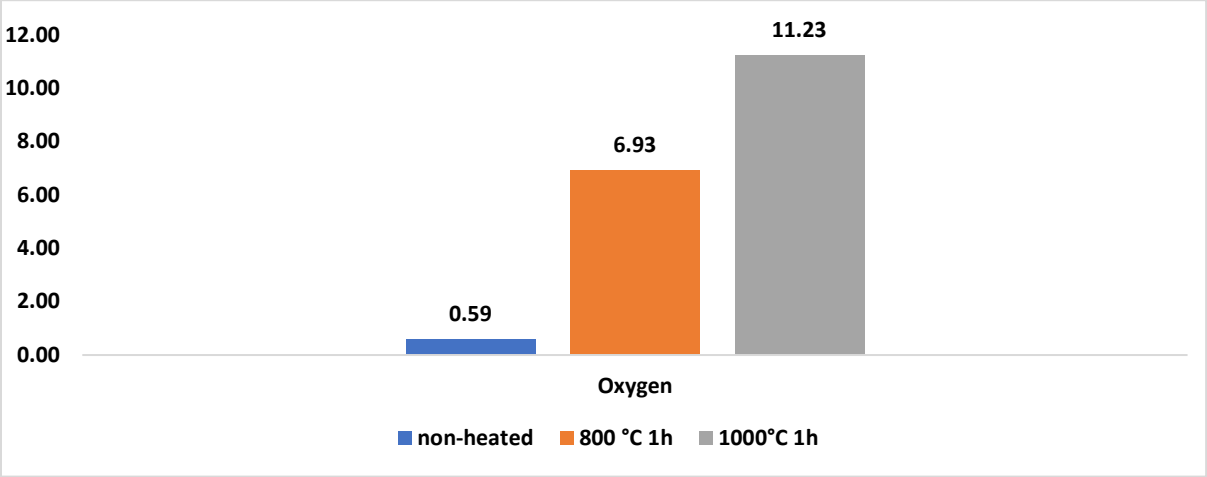

Figure 17 Oxygen content of the bare surfaces after experiencing different temperatures determined by SEM-EDX analysis

This phenomenon is an inconvenient as the aim is to enrich the sample in carbon, and not in oxygen. For further experiments, another surface that minimizes the oxygen contamination should be used.

2.3 Pyrolysis process – Effect of the heating time

As a third step, the effect of the heating time was investigated. On the previous part of the project, it was determined that a heating treatment at 500 °C for 1 h does not affect the structure, while at 800 °C and 1000 °C, a part or the totality of the tubes are degraded. Relatively high temperatures seem to provide too harsh conditions for the sample, even for a short heating time. Thus, for this part of the project, the experiments were focused on lower temperatures, but with longer heating times. More precisely, the experiments were performed at 500 °C and at 700 °C for 3 h. The experiments were repeated twice with the two different furnaces mentioned previously in order to see if the instrument that is used affects the reaction as well, and, if so, to determine which furnace is the most suitable for this project.

Figure 18 shows the different thermal cycle that were applied for the furnace located in the department of quantum matter physics. The experiment performed at 500 °C (**Figure 18A**) was conducted under argon atmosphere; the samples were heated at 600 °C/h until reaching 500 °C, heated for 3 h at this temperature, and then the furnace was turned off. Regarding the sample heated at 700 °C (**Figure 18B**), the samples were heated at 600 °C/h until reaching 600 °C, then at 300 °C/h until reaching 700 °C, heated for 3 h at this temperature, and then the furnace was turned off.

Figure 18 Illustration of the thermal cycle of the samples heated at A) 500 °C B) 700 °C in the furnace located in the department of quantum matter physics

Figure 19 shows the different thermal cycle that were applied for for the furnace located in the department of physical chemistry. The experiment performed at 500 °C (**Figure 19A**) was conducted under nitrogen atmosphere; the samples were heated at 100 °C/h until reaching 500 °C, heated for 3 h at this temperature, and then the furnace was cooled at r.t with a cooling rate of 100 °C/h. Regarding the experiment performed at 700 °C (**Figure 19B**), it was unfortunately conducted at atmospheric pressure and not under inert atmosphere due to a technical problem. The samples were first heated at 100 °C/h until reaching 700 °C, heated for 3 h at this temperature and then cooled down at a cooling rate of 100 °C/h.

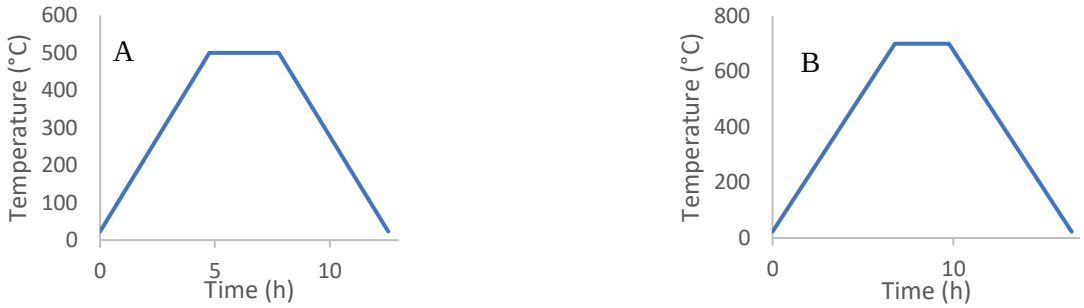

The samples were then characterized by their morphology and composition as was done previously. The next sections present the results that were obtained.

2.3.1 Transmission electron microscopy and Scanning electron microscopy

The morphology of the samples was determined by TEM and SEM. Regarding these TEM experiments, the samples were prepared and imaged by Kristina Jajcevic and used for comparison purposes. TEM grids of 20 nm of thickness were used in order to improve the quality of the images as suggested above.

Figure 19 Illustration of the thermal cycle of the samples heated at A) 500 °C B) 700 °C in the furnace located in the department of physical chemistry

First, the images obtained for the samples heated in the furnace located in the department of quantum matter physics (furnace 1) are presented, then the ones for the samples heated in the furnace located in department of physical chemistry (furnace 2), and finally, the comparison of both will be discussed.

Figure 20 shows transmission electron microscopy images and scanning electron microscopy images of samples heated at 500 °C for 3 h in furnace 1.

Concerning the results obtained by TEM, different regions are observed. In some parts, the shape of the LNTs is recognizable, but the tubes are disconnected (**Figure 20A**), while in other parts, the disconnected LNTs are visible as well, but in the tubes, small spherical structures of an averaged diameter of 18.94 ± 4.65 nm side by side are present (**Figure 20B an 20B-2**).

Regarding the results obtained by SEM, the system seems homogeneous. It can be observed that LNTs are present all over the surface (**Figure 20C**). By taking a closer look, it appears that the tubes are still connected and that their shape has not been altered by the heating process (**Figure 20D**). These results do not correspond to the ones obtained by TEM. However, it is

possible that other regions exist, as only a part of the sample is imaged by this technique, which means that some information is missing.

In view of their size and shape, the structures visible on image **Figure 22B-2** probably correspond to carbon dots, which are spherical carbon material with a diameter often smaller than 10 nm (larger sizes have been reported as well). The supposition of the formation of carbon dots is reasonable as this kind of materials can easily be synthesized via pyrolysis of organic compounds. Further investigation should be conducted to confirm the presence of carbon dots, and confirm the successful synthesis of carbon nanomaterials via pyrolysis of LNTs. Such structures can be characterized by TEM and AFM, but also through X-ray and Raman measurements as they present characteristic peaks. However, these specific peaks may be shifted when the carbon dot is doped with other elements such as azote and transition metals. This has to be taken into account if such an analysis is performed later on, as the sample may contain oxygen, azote and osmium

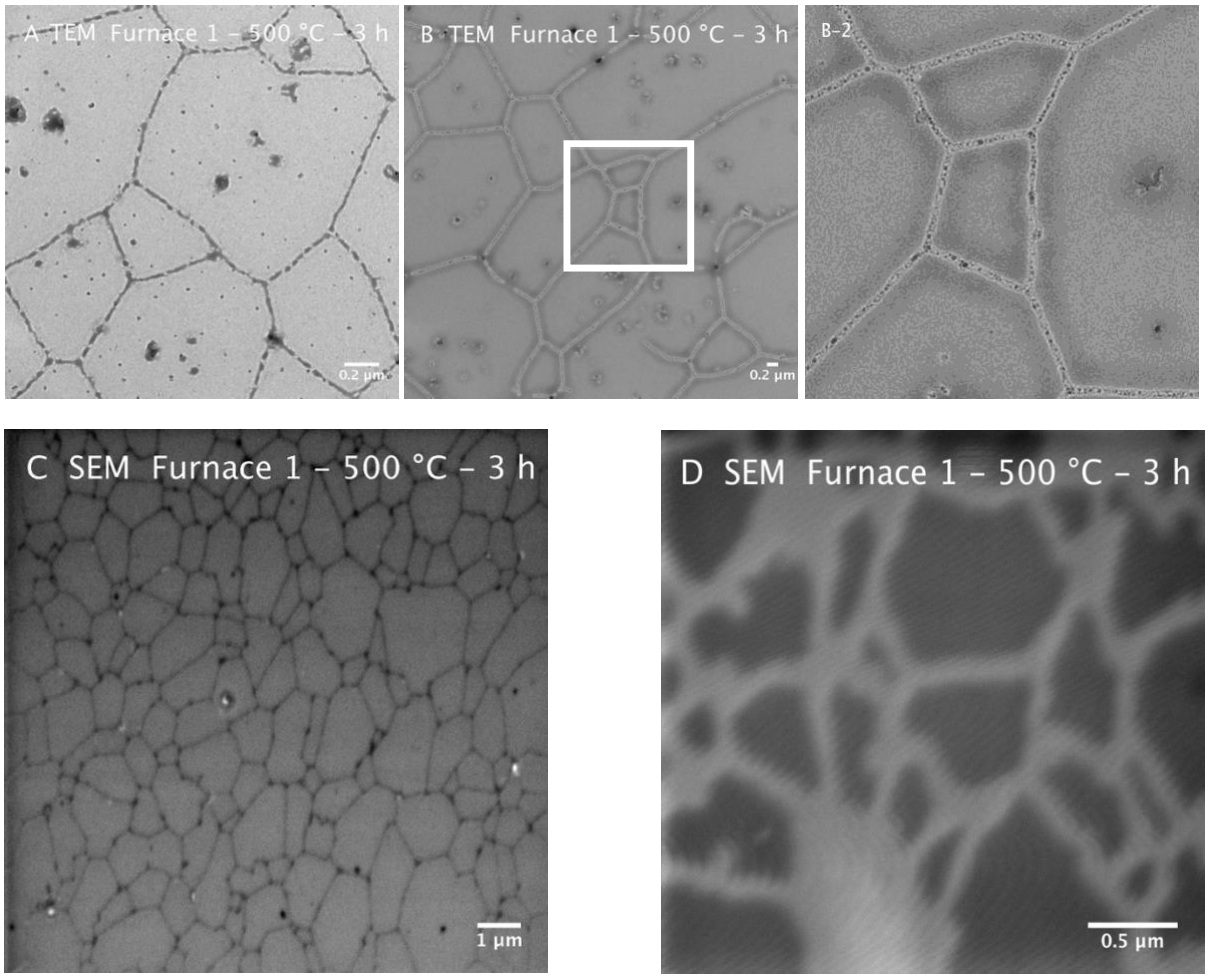

Figure 20 Transmission electron microscope images A), B) full image and B-2) zoom on the structures and scanning electron microscope images C) and D) of the samples after a heating process at 500 °C for 3 h in furnace 1.

Figure 21 shows transmission electron microscopy images and scanning electron microscopy images of samples heated at 500 °C for 3 h in furnace 2. It can be observed that the imaged structures are different from the ones visible when the samples are pyrolysed in the furnace 1.

Regarding the TEM results, no LNTs are visible anymore, but well aligned spherical structures forming a network similar to the LNTs' one is observed (**Figure 20A**). The diameter of the dots has a variable size; the average diameter is 74.28 ± 14.73 nm. So, the structure was destroyed by the pyrolysis process and the atoms reorganized themselves in these spherical shapes. These could possibly be carbon dots. However, the size of the observed dots is a bit too large to be considered as such material.

Regarding the SEM results, the initial location of the LNTs are visible, but by looking closely, it can be seen that some spherical structures are inside the former tubes (**Figure 20B**), meaning that the initial structure was degraded through the heating process. Some structures, that are less spherical than the ones observed by TEM, are visible, and their diameter is a little bit smaller: 61.74 ±14.53 nm, but this is still too large to consider the structure as carbon dots.

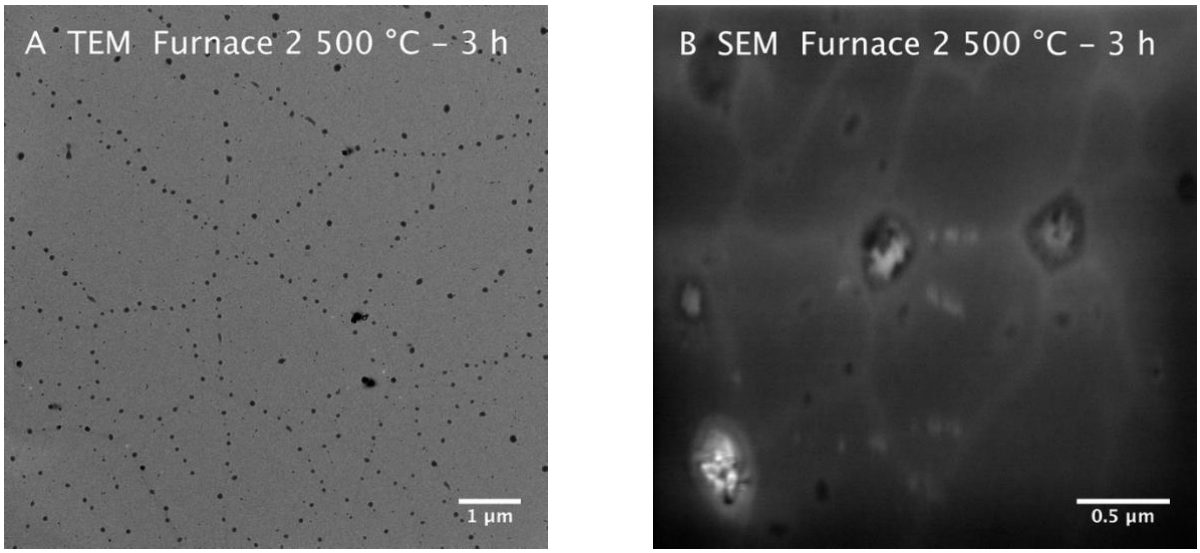

Figure 21 Transmission electron microscope images A) and scanning electron microscope images B) of the samples after a heating process at 500 °C for 3 h in furnace 2.

Figure 22 shows scanning electron microscopy images of samples heated at 500 °C for 3 h in furnace 1. Regarding the sample that is prepared on a TEM grid, it was not possible to put the grid in the furnace, because the holder might have contained contaminants that could have been released through heating, and then reacted with the sample. The grid being thin, it would probably have broken if no holder was used, so it was preferable not to use it at that moment. Thus, only the sample prepared on silicon wafer was introduced in the furnace and analysed.

Regarding the SEM results, different regions are observed. Some tubes are actually completely disconnected, and well aligned quasi spherical structures are visible (**Figure 22A**). The average size is 10.42 ± 1.91 nm, which is a small enough size to suggest the formation of carbon dots. The pattern formed by these dots looks like the former tube's network. Bigger structures, also disconnected and composed of small dots, are visible as well. These structures probably corresponded to the lipid block before the heating process. The shape and size of these small dots look like the morphology of carbon dots. A second region composed of these small structures that are folded on themselves, as previously discussed, is visible as well (**Figure 22B**). These fragmented structures form a network reminding the pattern of the LNTs network which suggests that the LNTs and the lipid blocks have been degraded.

Thus, it seems that these conditions of temperature and heating time allow the formation of carbon dots. However, other structures are also present in some regions., so other conditions should be investigated.

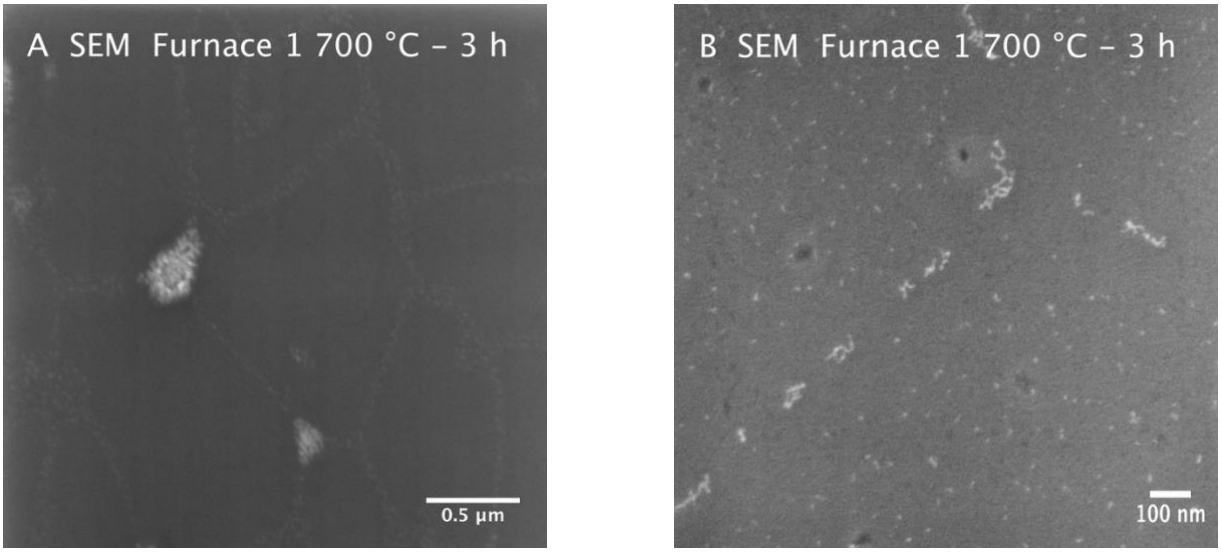

Figure 22 Scanning electron microscope images A) and B) of the samples after a heating process at 700 °C for 3 h in furnace 1.

Figure 23 shows transmission electron microscopy images and scanning electron microscopy images of samples heated at 700 °C for 3 h in furnace 2.

Regarding TEM results, there are no LNTs or spherical structures present on the surface (**Figure 23A**). A network of dark, compact and elongated and disconnected structures are visible. These structures look less compact and folded than the ones observed for the sample heated at 1000 °C for 1h. Also, dark crystals that were not present before are present all over the surface.

Regarding SEM results, only a few spots were imaged. In fact, as the furnace had some dust, the samples were protected by an aluminium sheet, and some aluminium was deposited on the surface because of the heat. Consequently, only one region was observed, but it is possible that other structures, which were hidden by the aluminium deposition, were present as well. The observed region presents a completely different structure from the one pictured for the sample treated in the other furnace. In this case, no LNTs are visible anymore (**Figure 23B**). Instead, some black dots are visible, that are probably what were previously the lipid blocks, linked by smaller disconnected dots, which in turn were probably the initial LNTs forming a network. These second kind of dots are bigger than the ones observed when the other furnace is used. These structures are probably not carbon dots in view of their (too big) size: 171.09 ± 31.20 nm.

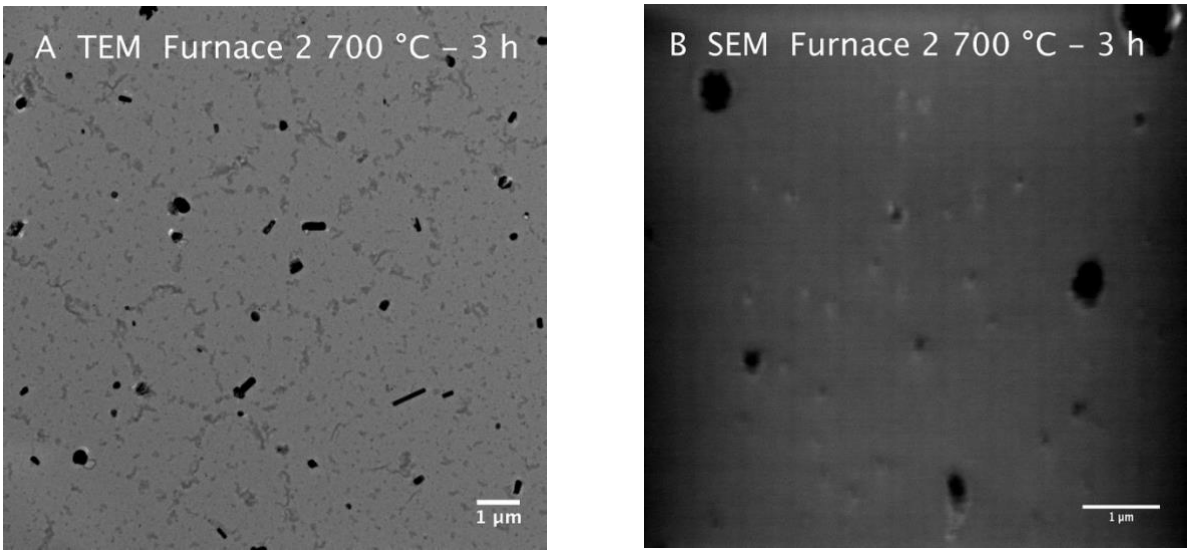

Figure 23 Transmission electron microscope images A) and scanning electron microscope images B) of the samples after a heating process at 700 °C for 3 h in furnace 2.

If one compares the morphologies observed with the two furnaces, it can be noticed that, even though the same temperature and the same heating time is applied, different results are obtained, which means that the instrument has an influence on the process. This difference is due to the fact that the heating rate and the cooling rate are different in both cases.

In fact, for the furnace 1, the heating rates are much more controlled than in the case of the furnace 2. Indeed, with the furnace 1, a ramp program can be set, and when approaching the targeted temperature, the rate can be decreased in order to have a better control of the temperature. Whereas with the second furnace, only one rate can be set. Additionally, the rates that can be set for the first furnace 1 are much faster than the ones of furnace 2, which allows to decrease the duration of the experiment. The cooling process is different as well; for the furnace 1, it is possible to turn it off right after the heating time, while for the furnace 2, a cooling rate has to be set. During this cooling process, the samples are still experiencing high temperatures. Thus, the duration for which the samples are effectively heated is different in both cases, which leads in turn to different results.

For future experiments, the furnace 1 should probably be preferred, as it is cleaner and because the temperatures are more controllable.

2.3.3 Scanning electronic microscopy with Energy Dispersive X-Ray

The composition was only investigated by SEM-EDX, because, even though the analysis is qualitative, it is the method that gave the most concluding results in the previous part of the project.

Only the samples heated in the furnace located in the department of quantum matter physics were analysed due to the aluminium deposition that would make the measurement unreliable. The measurements were performed at the same height and with the same parameters as the ones used for the previous analysis in order to make a reliable comparison between the effects of both the temperature and the heating time.

Figure 24 shows the atomic ratio for carbon, oxygen, nitrogen and osmium. As previously, nitrogen and osmium are not detected. Again, this might be due to the fact that the signal coming

from these two elements is hidden by the strong signal of the carbon and the oxygen. As previously, the sample is enriched in oxygen via pyrolysis process, and the effect becomes more important as the temperature increases.

Indeed, it can be seen that, for the sample heated at 500 °C for 3 h, the composition changes little compared to the non-heated sample. Even though the sample seems to be enriched in oxygen, the atomic ratios goes from 22.71 ± 1.97 % to 26.63 ± 4.91 %. Regarding the sample heated at 700 °C for 3 h, the sample is even more enriched in oxygen, 58.83 ± 0.51 %. This value is similar to the ones obtained for a heating process at 800 °C (60,57 %) and 1000 °C (61,55 %), both for 1 h. This means that, with lower temperatures and a longer heating time, approximately the same composition as with higher temperatures and shorter heating times is obtained. However, as seen in the previous analysis, the morphology is different.

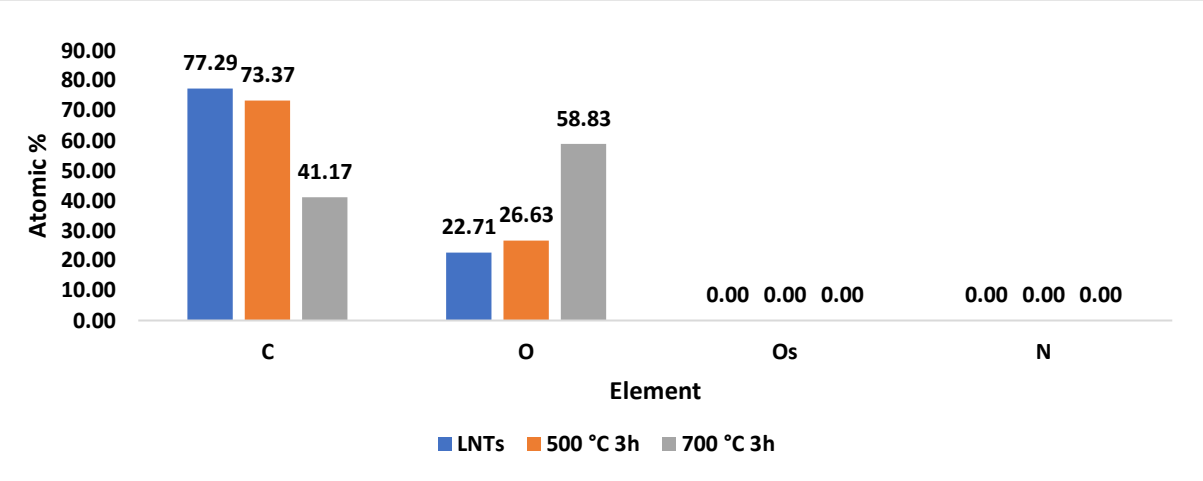

Figure 24 Atomic ratio of carbon, oxygen, osmium and nitrogen of the samples pyrolysed in furnace 1 determined by SEM-EDX analysis

The atomic ratio of oxygen at the surface of the silicon wafer was investigated as well. **Figure 25** shows the atomic ratio of oxygen obtained for the non-heated and heated bare surfaces. The same observation as for the previous analysis can be made; the higher the temperature, the higher the oxygen atomic ratio. In fact, the oxygen content at the surface is 0.59 ± 0.16 % for the non-heated sample, while it is 1.05 ± 0.15 % and 4.80 ± 1.14% respectively for the sample heated at 500 °C for 3 h and 700 °C for 3 h. However, it can be seen that these atomic ratios are smaller than the ones obtained for the previous experiments (6.93 % for the sample heated at 800 °C for 1 h and 11.23 % for the sample heated at 1000 °C for 1 h). Thus, it seems that applying lower temperatures and longer heating times, instead of high temperatures and short heating times, allows to minimize the oxygen contamination.

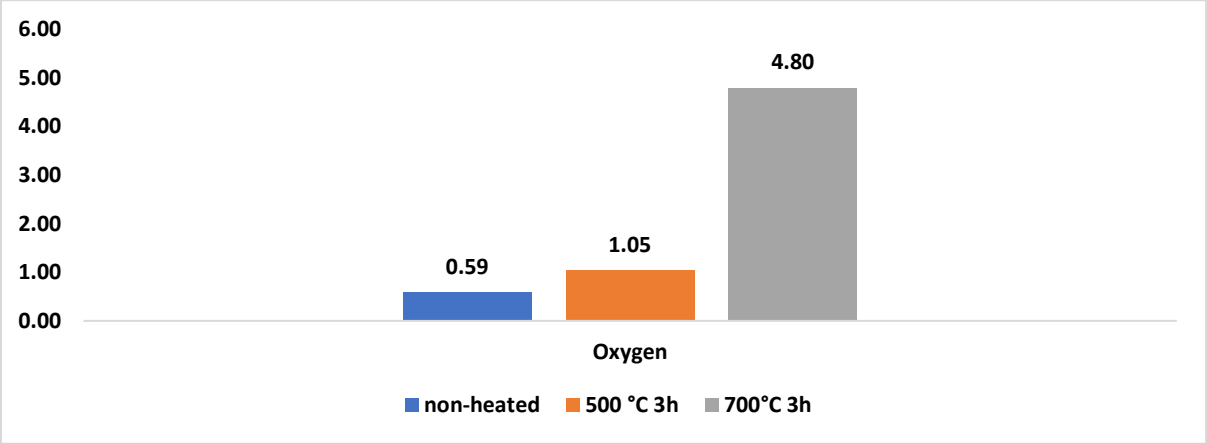

Figure 25 Oxygen content of the bare surfaces after experiencing different temperatures determined by SEM-EDX analysis

The determination of the composition being difficult due to the lack of instruments to characterize samples of such size, it was decided to directly apply heat treatment on the lipid block formed after sonication of the lipid solution, the size of which is in the centimetre scale.

2.3 Pyrolysis process of lipid blocks

For this last part of the project, the pyrolysis process was directly applied on a big lipid block in order to increase the quantity of material and facilitate the characterization of the sample after the heat treatment.

For these experiments, two different kinds of samples were used; dried lipids and fixed dried lipids. In the second case, the sample preparation was the following: the dried lipids have been resuspended with heated HEPES at 60 °C and then sonicated to detach the lipids from the vial's walls. After 4-5 minutes, a lipid block visible to the naked eye forms. Using a pipette, as much HEPES as possible without breaking the lipid block was removed. Then, the fixation solution was added and left for an incubation time of 30 minutes at 0 °C. The sample was then washed with HEPES and dried using ethanol and finally acetone as previously. **Figure 26** shows the lipid block before (**Figure 26A**) and after (**Figure 26B**) fixation. It can be seen that, after fixation, a powder is obtained and not so much material is left, as some of it is lost during the washing steps.

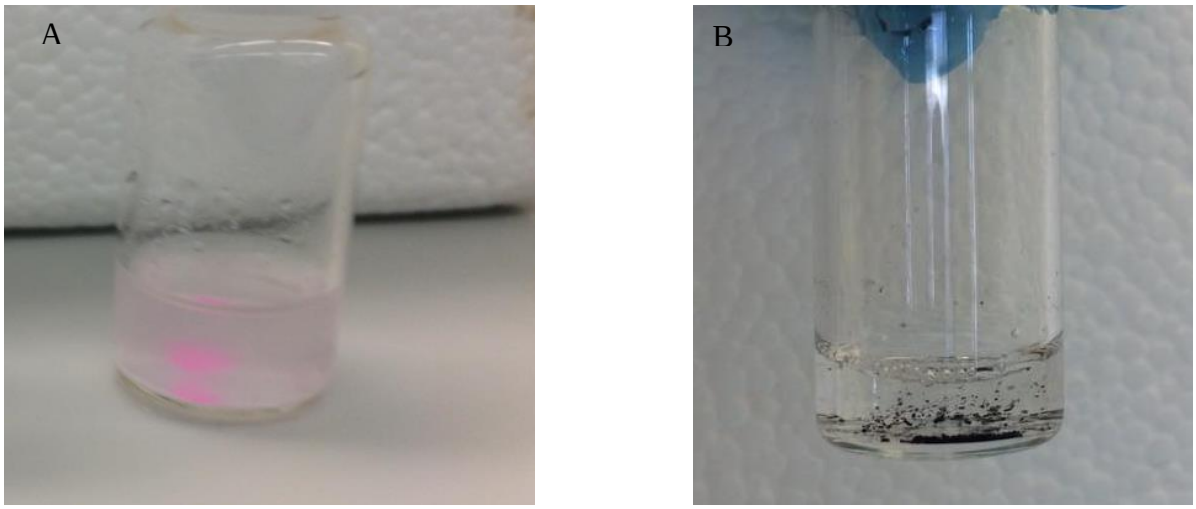

Figure 26 Illustration of the lipid blocks A) before fixation B) after fixation

The sample preparation was also performed with the triple quantities of DOPE, DOPE-Biotin and rhodamine in order to have even more material. The formed lipid block was quite large, so the fixation solution was left incubating overnight, as it takes some time for the solution to penetrate into the lipids. However, during the washing process, part of the lipid block detached and the inside of the block was still not fixed, which means that a longer time of incubation was needed. For further experiments, more than 24 h of incubation will be needed if such quantities of material are used, as the lipid block that is formed is quite thick. Thus, the experiments were performed with the samples prepared with the usual quantities of DOPE, DOPE-Biotin and rhodamine.

The samples were then pyrolysed in the furnaces located in the department of quantum matter physics at 500 °C for 3 h, with a heating rate of 600 °C/h and then quenched at the end of the heating process. The samples were characterized by ultra-Violet-Visible spectroscopy and infrared spectroscopy.

2.3.1 Ultra-Violet –Visible spectroscopy

Ultra-Violet-Visible (UV-VIS) spectroscopy is a method that allows to investigate the electronic transition of the sample. The sample is irradiated with a UV-VIS beam of intensity I_0 and the intensity I of the beam coming out of the sample is measured. If both beams have different intensities, it means that part of the light was absorbed by the sample in order to excite an electron that passes from one electronic state to another one of higher energy[30].

For this experiment, the samples were solubilized in methanol. Some particles were still in suspension, even after sonication, which means that the samples were not completely solubilized and that another solvent should be used next time.

The background and the solvent contribute to the signal, so both were measured individually and their signals were subtracted from the signal obtained for each sample in order to keep only the sample's contribution. Such arithmetic between the signals can be performed because the absorbance is an additive phenomenon.

Figure 27 shows the absorbance as a function of the wavelength obtained for the different samples. It can be observed that the dried lipids and the fixed lipid blocks have their electronic levels at different energies. Indeed, a peak at 279 cm^{-1} is observed only for the fixed sample and a peak at 563 cm^{-1} is only observed for the dried lipids. The other regions of the spectra is the same for all the samples. However, it is observed that both of these peaks disappear after the sample is heated, and that the spectrum is the same for both samples. This means that the electronic structure of the dried lipids and the fixed lipid blocks is changed and becomes the same when it experiences temperature like the ones that were applied.

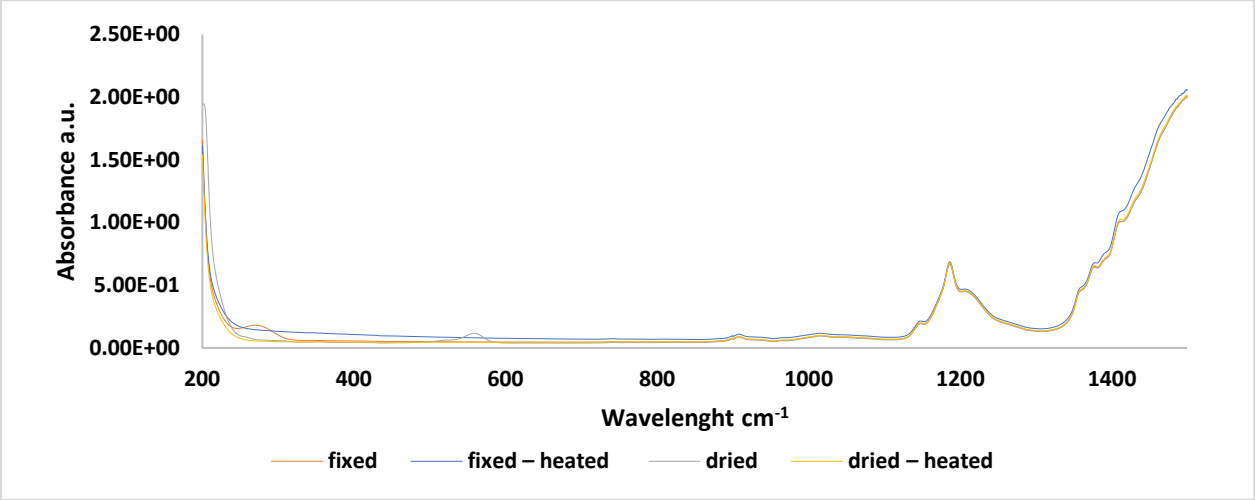

Figure 27 UV-VIS analysis of the samples before and after a heating treatment at 500 °C for 3 h

As nothing else could be deduced from this analysis, the structure was investigated by IR analysis to have more information.

2.3.1 Infrared spectroscopy

In order to have more information about the functional groups present on the structure, the sample has been analysed by infrared (IR) spectroscopy, a method allowing to investigate the composition of the sample by looking at the vibrations of the different bonds. The sample is irradiated with a beam of IR light of an intensity I_0 and the intensity I of the beam coming out of the sample is measured. If the intensities I_0 and I are different, it means that an absorption of frequency occurred. Such a phenomenon happens only when the frequency matches a vibrational frequency which is specific to each functional group. Thus, the sample composition at the surface can be investigated. However, not all the vibrations are detected, there is a selection rule: only the vibration implying a change of the dipole moment along the Cartesian coordinates are observable. This means that some information might be missing[31].

Figure 28 shows the absorbance as a function of the wavelength for each sample. The region above 1550 cm^{-1} is called the fingerprint region. The pattern observed in this region is specific to each molecule and is not used to determine the presence of a functional group. Thus, the region of interest to determine the functional groups is the one above 1500 cm^{-1}.

It can be observed that the intensities are relatively low, essentially for the heated samples. This is due to the fact that there was really little material left after the pyrolysis, so it was difficult to recover powder to make the analysis.

First, the results obtained for the dried and fixed samples before heating are compared. It can be seen that both have strong superposed peaks at 2925 cm^{-1} and at 2853 cm^{-1}. These peaks correspond respectively to an asymmetric and symmetric stretch of a C-H_2 bond. The peak at 720 cm^{-1} corresponds to a CH_2 deformation in the plane belonging to a carbon chain $(CH_2)_n$ with n greater than four, corresponding to the hydrophobic chain of DOPE. The peak around 2363 cm^{-1} present in both cases is specific to an asymmetric stretch of CO_2 . The peaks at 1723 cm^{-1} and the two bands between 1166 cm^{-1} and 1269 cm^{-1} show the presence of acyclic saturated esters, which is actually a functional group present in DOPE. The peaks respectively correspond to an elongation of a C=O bond and to an elongation of a C-O bond. Even if both graphics are similar, there are some differences. Around 3300 cm^{-1}, a large and strong peak is present for

the dried sample, while a sharper one is present for the fixed one, which means that the structure is different. A hypothesis is that this peak is related to the elongation of a O-H bond of an intramolecular hydrogen bond for the dried sample, while it could correspond to the elongation of a =N-H bond of an imine group introduced during the fixation step. The small peak present at 1664 cm^{-1} for the fixed sample confirms the presence of an imine group, as it can correspond to the elongation of a C=N bond. For the dried sample, peaks at 1696 cm^{-1} and at 1640 cm^{-1} correspond to the deformation in the plane of a N-H bond and to the elongation of a C=C bond, showing the presence of amine and alkene groups. These peaks are not present for the fixed sample as these groups transformed through a chemical reaction during the fixation step.

Regarding the fixed and heated sample, the peaks related to CH_2 groups are still visible even though the intensity is quite small compared to the non-heated sample. The peak corresponding to CO_2 is still present as well. However, no peaks are visible for the imine and ester groups.

Regarding the sample of the dried and heated lipids, it can be seen that the peaks of the hydrogen bond, CH_2 and ester groups are not present anymore, which means that the new structure does not contain these functional groups. Only the peak related to the CO_2 group is still present.

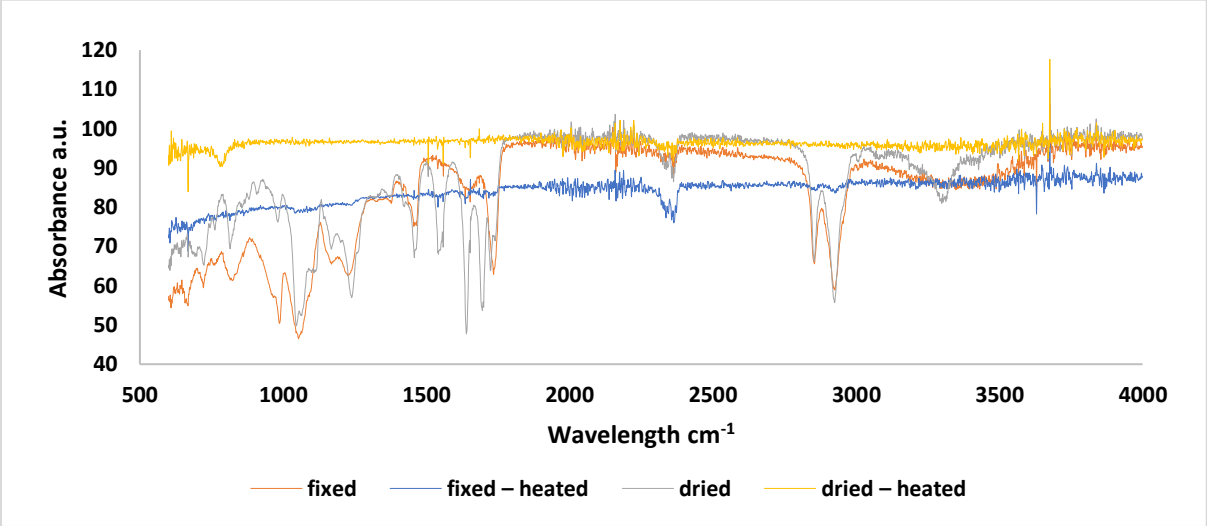

Figure 28 IR analysis of the lipid blocks before and after a heating treatment at 500 °C for 3 h

Through this experiment, it is shown that the structure is different for the fixed and dried samples, which was expected as the fixation step changes the chemical structure.

Also, by a heating treatment the structure experiences some changes; imine and the ester groups are not present anymore. The CH_2 group is only visible for the fixed sample after heating. Only the CO_2 signal is still present in both cases after the heating process.

3. Conclusion

In conclusion, the potential of the pyrolysis of lipid nanotubes to synthesize carbon nanomaterials was investigated, and it was found not to be conclusive for the moment.

Once the protocol to form the LNTs was established, the effect of the temperature was tested first. By TEM and SEM, it was shown that the LNTs were degraded when high temperatures such as 1000 °C were applied, even for a short time (1 h), while low temperature (500 °C) and a short heating time affected little the system. For intermediate temperatures, such as 800 °C, the system was not homogeneous; different structures were observed.

Regarding the composition, it was challenging to find an efficient method to characterize the samples. The signal was either too low to be significant or the instrument was not suitable for surfaces. Despite this, some information was collected by SEM-EDX. It was concluded that the sample was enriched in oxygen through a heating treatment, and this phenomenon increases along with the temperature. This phenomenon is probably due to the silicon wafer, which is contaminated by oxygen by entering into contact with air. This oxygen might have been liberated through the heating treatment and react with the sample.

Then, the effect of the heating time was investigated. It was shown that carbon dots can probably be formed by heating the sample at 500°C and 700 °C for 3 h. The size and the shape are good indicators in order to recognize this type of carbon nanomaterials. However, the structure is not observed all over the surface, meaning this path of synthesis is not well controlled. Also, the control of the temperature is crucial for the process. Indeed, depending on the instrument that is used, the heating and cooling ramp is different, leading to different size and arrangement. It seems that fast heating and cooling are needed for a heating time of 3 h, otherwise other folded structures are obtained. Thus, the furnace located in the department of quantum matter physics seems to be more suitable for this project.

Regarding the composition, the same observations were made; the sample was enriched in oxygen, and the higher was the applied temperature, the higher was the atomic ratio of oxygen. However, it was shown that applying low temperatures for long times allows to minimize this enrichment compared to high temperatures applied for short times.

In view of the difficulties to obtain a relevant signal for the composition, lipid blocks were pyrolysed. It was observed that the electronic structure and the chemical structure were changed after the heating treatment. Regarding the IR analysis, the CO_2 and the CH_2 for the fixed sample remained after pyrolysis. However, it has not been determined if a carbon nanomaterial was synthesised or not, or even if the samples were enriched in carbon as no SEM-EDX analysis could be performed (the instrument cannot be used for powders).

Consequently, it seems that carbon nanomaterials, more precisely carbon dots, can be synthesised through pyrolysis of LNTs. However, the synthesis is not controlled at all. Indeed, structures other than carbon dots are generated at the same time. Also, the diameter varies depending on the conditions, and the organisation of the dots changes as well. In fact, the dots were either closed to one another and randomly placed or they were well aligned.

The experiments should be performed again to see the reproducibility of the process. Other temperatures and/or heating times should also be investigated in order to improve the synthesis of carbon dots via LNTs pyrolysis and to have a better control of their size and morphology.

4. Experimental Section

4.1 Surface cleaning

In order to avoid any contamination, glass coverslips 24X24 mm and silicon wafers were first cleaned with acetone, with isopropanol and then with milli-Q water. Between each step, the surfaces were sonicated for 10 min. The surfaces were finally dried with a stream of nitrogen before going to the furnace for at least 2 h at 60 ° C.

4.2 Buffer solution preparation

The buffer solution was prepared by dissolving 4-(2-hydroxyethyl) piperazine-1-ethanesulfonic acid (HEPES) (10 mM) and NaCl (150 mM) in distilled water. The pH was then adjusted to 7.4 using 6M NaOH. Finally, the solution was filtered to make sure that there were no contaminants.

4.3 Preparation of polymer solutions

PEI

The polymer solution was prepared by dissolving polyethyleneimine (PEI) in HEPES at 0.1 mg/ml concentration.

PLL-g-PEG: PLL-g-PEG-Biotin

The polymer solution was prepared from poly(L-lysine)-*graft*-poly(ethylene glycol) (PLL-*g*-PEG) and poly(L-lysine)-*graft*-poly(ethylene glycol) biotin (PLL-*g*-PEG-Biotin). Both of them were dissolved in milli-Q water at a concentration of 0.1 mg/m and then added in the same flask in a ratio of 10:1 PLL-*g*-PEG: PLL-*g*-PEG-Biotin.

4.4 Preparation of polymer-coated surfaces

Glass coverslips, silicon nitride surfaces and silicon wafers were activated through oxygen plasma activation (TePla IoN 3Mz oxygen plasma machine). During this process, oxygen free radicals bound to the material surface, facilitating the polymer adhesion. Polydimethylsiloxane (PDMS) was cut into squares with a well in the middle. The piece of PDMS was then adhered at the middle surface to accommodate the sample.

PEI-coated surface

Then 50 μL of PEI were added in the well, and the solution was left incubated for 30 min at r.t. The surface was washed 15 times with HEPES buffer (100 μL).

PLL-g-PEG-Biotin-coated surface

Then 50 μL of PLL-*g*-PEG/PLL-*g*-PEG-Biotin solution was added in the well, and the solution was left incubated 30 min at r.t. The surface was washed 15 times with milli-Q water. Then

50 μL of streptavidin (50 μg/ml in H_20) were added followed by 30 min incubation at r.t. The surface was washed 15 times with milli-Q water again.

4.5 Preparation of lipid solutions

DOPE

The lipid solution was prepared from 25 mg/mL 1,2-dioleoyl-*sn*-glycero-3-phosphoethanolamine (DOPE) stored in chloroform. In order to be able to image the LNTs by fluorescent microscopy, a fluorophore-tagged lipid (Rhodamine-PE) was added at a concentration of 1%. The solution was dried under vacuum for at least 2 h. The lipids were then resuspended in HEPES to a final concentration of 1mg/mL and then sonicated until the lipids detached from the vial's wall.

DOPE-Biotin

The lipid solution was prepared from 25 mg/ml 1,2-dioleoyl-*sn*-glycero-3-phosphoethanolamine (DOPE) and 10 mg/ml 1,2-dioleoyl-*sn*-glycero-3-phosphoethanolamine-N-(cap biotinyl) (sodium salt) (DOPE-Biotin) stored in chloroform. Both solutions were added in the same vial in a ratio of 96:4 DOPE: DOPE-Biotin. In order to be able to image the LNTs by fluorescent microscopy, a fluorophore-tagged lipid (Rhodamine-PE) was added at a concentration of 1%. The solution was dried under vacuum for at least 2 h. The lipids were then resuspended in HEPES to a final concentration of 1mg/mL and then sonicated until the lipids detached from the vial's wall.

4.6 Chemical fixation of LNTs

The solution used to fix the sample was prepared from stock solutions of cacodylate buffer at pH 7.4, 25 % glutaraldehyde and 4 % osmium tetroxide. Then stock solution of 2.5 % glutaraldehyde and 1 % osmium tetroxide in cacodylate buffer was prepared. Osmium tetroxide and glutaraldehyde solutions were mixed in the same flask respectively in a ratio of 2:1 and placed in an ice bath. After removing the 100 μl of liquid from the wells, 100 μL of the fixation solution were added, and left incubated for 30 min in an ice bath. The fixation solution was then removed and the samples were washed 10 times with HEPES buffer. The samples were dehydrated with successive increasing solutions of ethanol (15, 30, 50, 80, 95 and 100 %) for 2 minutes at each step. Finally, 100 μL of 100 % acetone solution were added for 2 minutes and the samples were air dried to finalize the dehydration.

5. References

1. K. Siraj, T. E. Tesema and N. I. Alvi, *J Chem Applied Biochem.*, 2014, 1, 1-6

2. N. J. Coville, S. D. Mhlanga, E. N. Nxumalo and A, Shaikjee, *S. Afr. J. Sci*, 2011, 107, 1-15

3. T. Shimizu, M. Masuda, and H. Minamikawa, *Chem. Rev.*, 2005, 105, 1402-1443

4. K. Sugihara, M. Chami, I. Derényi, J. Vörös and T. Zambelli, *Acs Nano*, 2012, 6, 6626-6632

5. P. Avouris and C. Dimitrakopoulos, *Mater. Today*, 2012, 15, 86-97

6. M. Mojica, J. A. Alonso and F. Méndez, *J. Phys. Org. Chem.*, 2013, 26, 526-539.

7. I. Rašović, *Mater. Sci. Technol.*, 2017, 33, 777-794

8. T. Grattia, E. Mennaa, M. Meneghettia, M. Magginia, A. Petrozzab and F. Lambertia, *Nano Energy*, 2017, 41, 84-100

9. J. Nelson, *Mater. Today*, 2011, 14, 462- 470

10. W. Zhai, N. Srikanth, L. B. Kong and K. Zhou, *Carbon*, 2017, 119, 150-171

11. S. Z. Mousavi, MD, S. Nafisi and H. I. Maibacha, *Nanomedicine*, 2017, 13, 1071-1087

12. A. Eatemadi, H. Daraee, H. Karimkhanlool, M. Kouhi, N. Zarghami, A. Akbarzadeh, M. Abasil, Y. Hanifehpour and S. W. Joo, *Nanoscale Res. Lett.*, 2014, 1-13

13. K. Moothi, G. S. Simate, R. Falcon, S, E, Iyuke and M. Meyyappan, *Langmuir*, 2015, 31, 9464-9472

14. W. Yuan, Y. Zhang, L. Cheng, H. Wu, L. Zheng andD. Zhao, *J. Mater. Chem. A*, 2016, 4, 8932-8951

15. C. Tîlmaciu and M. C. Morris, *Front. Chem.*, 2015, 3, 1-21

16. L. Peng, Z. Zhang and S. Wang, *Mater. Today*, 2014, 17, 433-442

17. Z. L. Wu, Z. X. Liu and Y. H. Yuan, *J. Mater. Chem. B*, 2017, 5, 3794-3809

18. X. Han, S. Li, Z. Peng, A. O. Al-Yuobi, A. S. O. Bashammakh, M. S. El- Shahawi and R. M. Leblanc, *J. Oleo Sci.*, 2016, 65, 1-7

19. M. Tuerhong, X. Yang and Y. Xue-Bo, *Chin. J. Anal. Chem.*, 2017, 45, 139-150

20. C. E. Chivers, A. L. Koner, E. D. Lowe and M. Howarth, *Biochem. J.*, 2011, 435, 55-63

21. K. Jajcevic, M. Chami and K. Sugihara, *Small*, 2016, 12, 4830-4836

22. J. H. Bowes and C. W. Cater, *J. R. Microsc. Soc.*, 1966, 85, 193-200

23. J. C. Riemersma, *Biochim. Biophys. Acta.*, 1968, 152, 718-727

24. R. F. Egerton, *Springer, Cham*, 2016, 5-6, 55-88, 121-147

25. N. Ahlawat, *IJCSMC*, 2014, 11, 680-685

26. P. Verma, *Chem. Rev.*, 2017, 117, 6447-6466

27. A. Wlodawer, W. Minor, Z. Dauter and M. Jaskolski, *FEBS J.*, 2008, 275, 1-21

28. A. V. Girão, G. Caputo and M. C. Ferro, *Compr. Anal. Chem.*, 2017, 75, 153-168

29. R. L. Sandberg, D. D Allred, A. L. Jackson, J. E. Johnson, W. Evans, W. Evans, T. Doughty, A. E. Baker, K. Adamson, A. Jacquier, and R. E. Robinson, *SVC*, 2004, 47, 368-376

30. R. S. Shah, R. R. Shah, R. B. Pawar, P. P. Gayakar, *IJIPLS*, 2015, 5, 490-505

31. R. S. McDonald, *Anal Chem.*, 1982, 54, 1250-1275

I hereafter certify that every statement of this report originating from another source than my personal thoughts has been attributed to its legitimate source, and that every statement directly copied from another source is explicitly mentioned between quotes.

Wendy Nogueira